O-Nucleoside, S-Nucleoside, and N-Nucleoside Probes of Lumazine Synthase and Riboflavin Synthase

Arindam Talukdar,[†] Yujie Zhao,[†] Wei Lv,[†] Adelbert Bacher,[‡] Boris Illarionov,[‡] Markus Fischer,[‡] and Mark Cushman*,[†]

[†]Department of Medicinal Chemistry and Molecular Pharmacology, College of Pharmacy, and The Purdue Center for Cancer Research, Purdue University, West Lafayette, Indiana 47907, United States

[‡]Institute of Biochemistry and Food Chemistry, Food Chemistry Division, University of Hamburg, D-20146 Hamburg, Germany

S *Supporting Information*

ABSTRACT: Lumazine synthase catalyzes the penultimate step in the biosynthesis of riboflavin, while riboflavin synthase catalyzes the last step. O-Nucleoside, S-nucleoside, and N-nucleoside analogues of hypothetical lumazine biosynthetic intermediates have been synthesized in order to obtain structure and mechanism probes of these two enzymes, as well as inhibitors of potential value as antibiotics. Methods were devised for the selective cleavage of benzyl protecting groups in the presence of other easily reduced functionality by controlled hydrogenolysis over Lindlar catalyst. The deprotection reaction was performed in the presence of other reactive functionality including nitro groups, alkenes, and halogens. The target compounds were tested as inhibitors of lumazine synthase and riboflavin synthase obtained from a variety of microorganisms. In general, the S-nucleosides and N-nucleosides were more potent than the corresponding O-nucleosides as lumazine synthase and riboflavin synthase inhibitors, while the C-nucleosides were the least potent. A series of molecular dynamics simulations followed by free energy calculations using the Poisson−Boltzmann/surface area (MM-PBSA) method were carried out in order to rationalize the results of ligand binding to lumazine synthase, and the results provide insight into the dynamics of ligand binding as well as the molecular forces stabilizing the intermediates in the enzyme-catalyzed reaction.
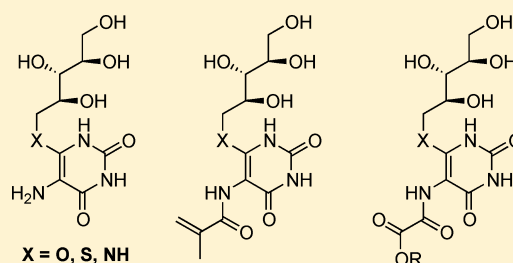
INTRODUCTION

Riboflavin, also known as vitamin B_2, is the central component of the cofactors FAD and FMN and is therefore required for a wide variety of cellular processes. It plays a key role in energy production and is required for the metabolism of fats, carbohydrates, and proteins. Animals, including humans, obtain it from their diet, while a variety of pathogenic Gram-negative bacteria, including *Escherichia coli* and *Salmonella typhimurium*, lack an efficient riboflavin uptake system and are therefore absolutely dependent on endogenous synthesis of this vitamin.[1−4] The riboflavin biosynthesis gene *ribB* has recently been shown to play an essential role in different *Salmonella* disease models.[5,6] Since animals lack the riboflavin biosynthetic pathway, inhibitors of the pathway should be selectively toxic to the pathogen and not the host. A detailed understanding of the structure and mechanism of the enzymes involved in the biosynthesis of riboflavin is essential for the rational design of enzyme inhibitors with antibacterial activity.

Lumazine synthase and riboflavin synthase catalyze the last two steps in the biosynthesis of riboflavin (Scheme 1). The initial steps in the biosynthesis of riboflavin lead from GTP to the pyrimidinedione **1**.[7−15] Lumazine synthase catalyzes the condensation of 3,4-dihydroxy-2-butanone 4-phosphate (**2**)[16−18] with 5-amino-6-D-ribitylamino-2,4(1*H*,3*H*)-pyrimidinedione (**1**) yielding 6,7-dimethyl-8-D-ribityllumazine (**3**).[19,20] The four-carbon phosphate moiety **2** originates from the

pentose phosphate pool by the loss of C-4. The riboflavin synthase-catalyzed dismutation of two molecules of 6,7-dimethyl-8-D-ribityllumazine (**3**) results in the formation of one molecule of riboflavin (**4**) and one molecule of the substituted pyrimidinedione **1**, which can be recycled by lumazine synthase.[21−29] The pyrimidinedione derivative **1** is therefore both a substrate of lumazine synthase and a product of riboflavin synthase, and analogues of **1** could therefore conceivably bind to and inhibit both lumazine synthase and riboflavin synthase.

The mechanism of the reaction catalyzed by lumazine synthase has not been completely elucidated. The currently proposed mechanism outlined in Scheme 2 involves initial Schiff base formation between the four-carbon carbohydrate **2** and the pyrimidinedione derivative **1**, resulting in the imine **5**, which eliminates phosphate to form the enol **6** (Scheme 2). Tautomerization of the enol **6** to the ketone **7**, followed by the addition of the secondary amino group to the ketone, leads to the formation of the covalently hydrated lumazine **10**. Elimination of water yields the 6,7-dimethyl-8-D-ribityllumazine (**3**). A redox disproportionation reaction of two molecules of **3**, followed by a 4 + 2 cycloaddition reaction and two elimination reactions, has recently been advanced in order to explain the conversion of two
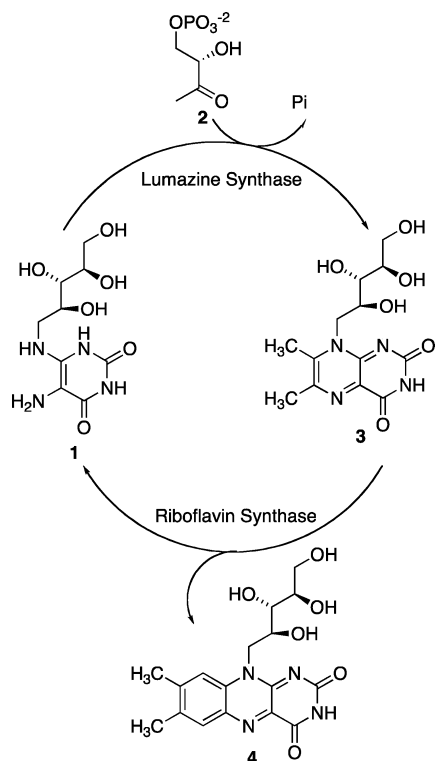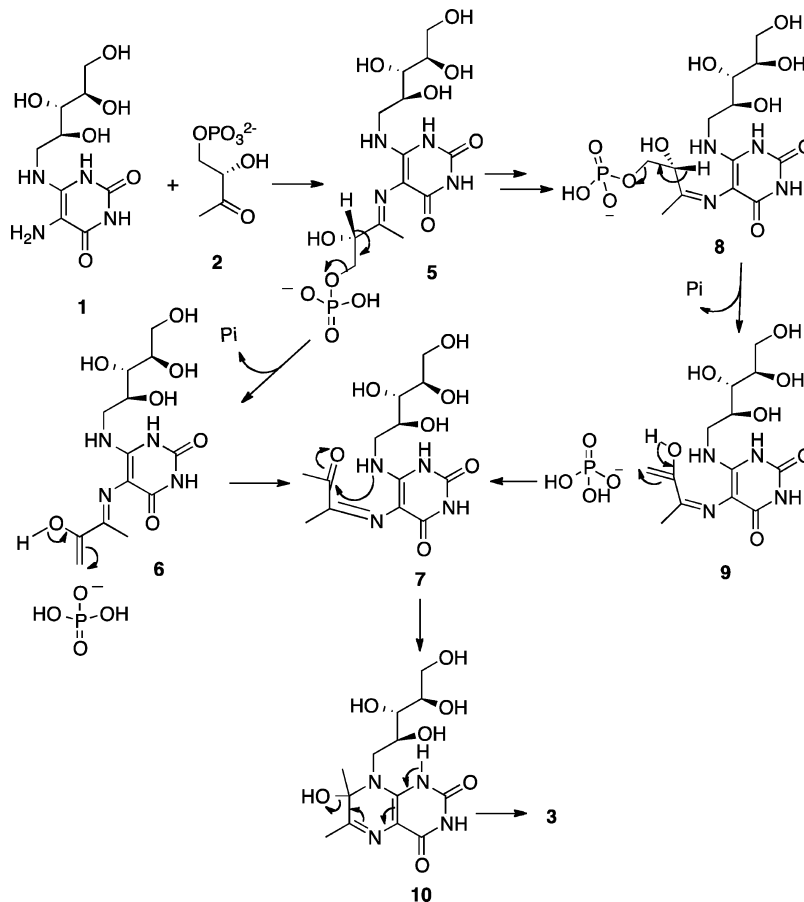
Scheme 1

molecules of the lumazine **3** to one molecule of riboflavin (**4**) and one molecule of the pyrimidinedione **1** (Scheme 3).[30]

X-ray crystallography of complexes of the purinetrione inhibitor **15** (PDB code: 1W19) and the phosphonate analogue **16** (PDB code: 1NQW) with lumazine synthase has established that the phosphate of the hypothetical Schiff base initially binds far away from the ribityl side chain as depicted roughly in chemical structure **5** (Chart 1).[31] Although the mechanism outlined in Scheme 2 is certainly very reasonable, the details of the pathway, such as the timing of phosphate elimination relative to the conformational reorganization of the side chain to allow cyclization, remain unknown.[32] For example, it has been proposed that the whole phosphate side chain rotates toward a cyclic conformation **8** with assistance from the enzyme before phosphate elimination and dehydration occur to form the cis Schiff base **7** directly (Scheme 2).[31] The possible initial formation of a thermodynamically less stable cis Schiff base, or the isomerization of the trans Schiff base **17** to the cis Schiff base **7**, has not been established. By a semiempirical approach, the energy barrier for the **17** to **7** isomerization was calculated to be 19.6−21 kcal/mol.[33] More recently, as a result of the temperature-dependent pre-steady-state kinetic experiments of lumazine synthase from *Aquifex aeolicus*, it was proposed that one of the subsequent steps occurring after phosphate elimination and tautomerization is the rate-determining step.[34,35]

Ligand Design. In order to gain insight into the structural change of the Schiff base side chain occurring after formation of intermediate **5**, metabolically stable substrate analogues are
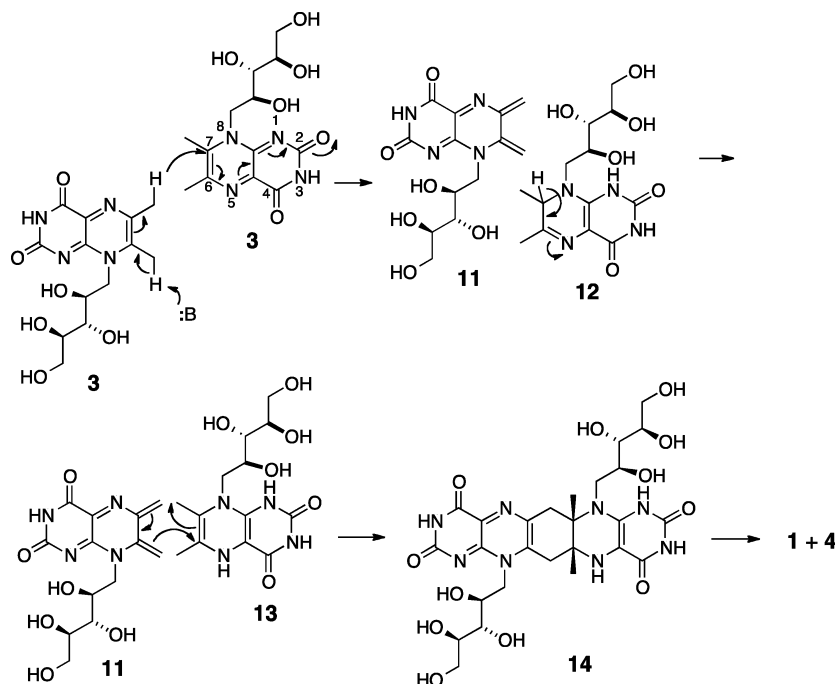
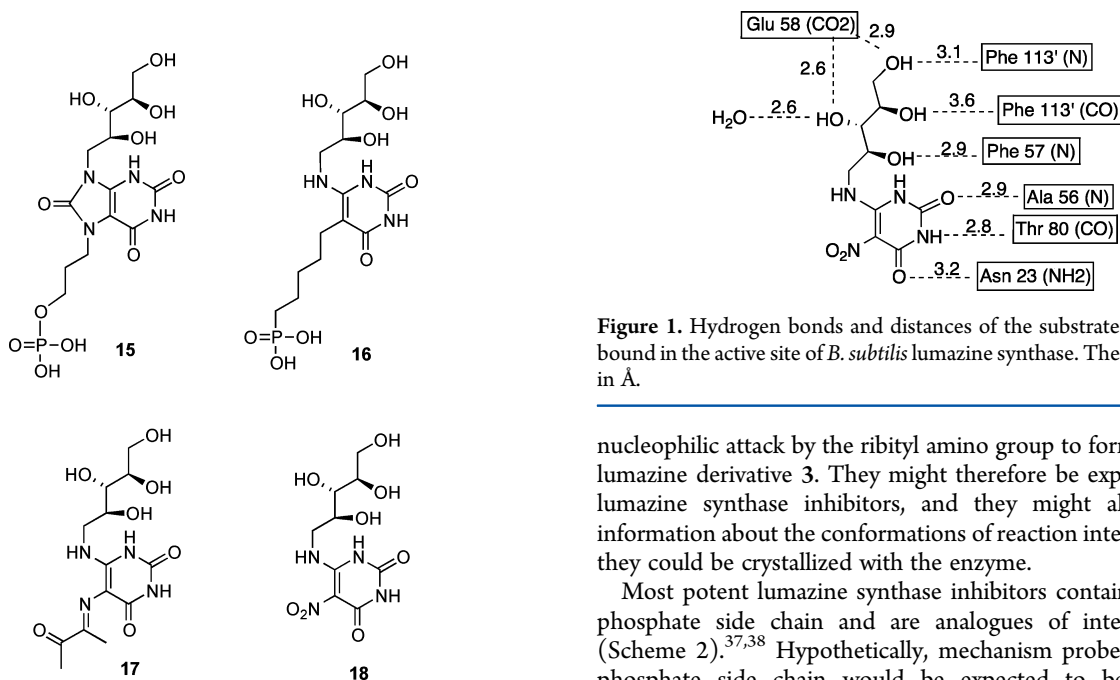**Scheme 2**

Scheme 3

Chart 1

Figure 1. Hydrogen bonds and distances of the substrate analogue **18** bound in the active site of *B. subtilis* lumazine synthase. The distances are in Å.

necessary that would allow Schiff base formation but would not allow the cyclization to proceed. The crystal structure of analogue **18** (PDB dode: 1KYY) bound to *Bacillus subtilis* lumazine synthase[36] has revealed that the ribitylamino nitrogen has no obvious direct role in binding the ligand to the enzyme (Figure 1), suggesting that the replacement of the nitrogen with another atom might not affect binding to the enzyme.

Replacement of the nitrogen atom of the ribitylamine side chain with oxygen, sulfur, or carbon would not be expected to produce gross changes in the orientation of ribityl chain of **18** (Figure 1), and the resulting compounds could possibly bind to both lumazine synthase and riboflavin synthase. They obviously could not complete the catalytic cycle as they cannot undergo the nucleophilic attack by the ribityl amino group to form the cyclic lumazine derivative **3**. They might therefore be expected to be lumazine synthase inhibitors, and they might also provide information about the conformations of reaction intermediates if they could be crystallized with the enzyme.

Most potent lumazine synthase inhibitors contain a C3–C5 phosphate side chain and are analogues of intermediate **5** (Scheme 2).[37,38] Hypothetically, mechanism probes without a phosphate side chain would be expected to be moderate lumazine synthase inhibitors compared to the more potent ones with a phosphate side chain because the phosphate binds to Arg, Thr, Ala, Gln, and Ser residues in the active sites of lumazine synthases isolated from a variety microorganisms.[31,32,39–43] Accordingly, intermediate **5** is likely to have a higher affinity for the enzyme than intermediates **6** or **7**. Enol **6** is an intermediate from the hypothetical reaction mechanism after phosphate cleavage. In the present study, metabolically stable analogues of lumazine synthase substrate **1** and reaction intermediate **6** were designed.

The proposed intermediate **6** is a Schiff base. Schiff bases are not stable under acidic and reductive conditions. Bioisosteres **19** and **20** were therefore designed as metabolically stable analogues of the Schiff base **6** (Chart 2). These amides have partial double

Chart 2
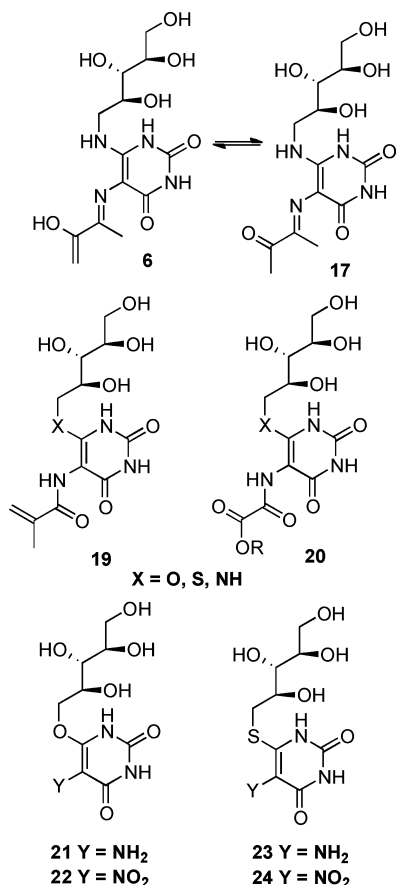
bond character between the amide nitrogen and the carbonyl carbon. Compound **19** has a methacroyl side chain attached to 5-amino-6-ribitylamino-1*H*-pyrimidine-2,4-dione, which resembles the intermediate **6**.

Compounds **21**−**24** mimic the intermediate **1**, which is a substrate of the lumazine synthase-catalyzed reaction and a product of the riboflavin synthase-catalyzed reaction. These compounds therefore have the potential to inhibit both enzymes.

There are indeed many common features of riboflavin synthase and lumazine synthase, and the dual inhibitor concept has, in principle, a strong theoretical basis. In fact, the sequences and structures of riboflavin synthases of Archaea closely resemble those of 6,7-dimethyl-8-ribityllumazine synthase, as evidenced by the crystal structure of a pentameric *Methanocaldococcus jannaschii* riboflavin synthase in complex with a substrate analogue.[44]

Molecular Modeling of *O*- and *S*-Nucleosides. A 2.4 Å resolution X-ray structure is available of the substrate analogue **18** (PDB code: 1KYY)[36] complexed with *B. subtilis* lumazine synthase (Figure 1). The structure allows the construction of hypothetical models of the binding of **21**−**24** to lumazine synthase (Figure 2), which were produced by docking these compounds into the active site of *Mycobacterium tuberculosis* lumazine synthase. Docking was performed with GOLD (BST, version 3.0, 2005; for details, see the Experimental Section). The energies of the complexes were minimized using the MMFF94s force field while allowing the ligand and the protein structure contained within a 6 Å diameter sphere surrounding the ligand to remain flexible with the remainder of the protein structure frozen. The calculated structures of **21**−**24** bound to lumazine synthase suggest that these inhibitors bind in the active site in an almost identical fashion to **18** (Figure 2).

■ RESULTS AND DISCUSSION

Synthesis of *O*-Nucleosides. Since both the ribityl hydroxyl groups and the pyrimidinedione ring have the potential to be alkylated, the attachment of a side chain on the amino group at C-5 of the pyrimidinedione moiety required that the ribityl substituent and the pyrimidinedione ring be generated in protected forms. The synthesis of the protected ribitol **26** started from D-ribose as previously described.[45] Treatment of chloropyrimidine **25** with the ribitol derivative **26** was carried out in the presence of the hindered base LiHMDS. The reaction was attempted in the presence of NaH and BuLi, but LiHMDS gave the best result. The reaction proceeded in 71% yield to afford the desired product **27**.

The removal of the isopropylidene groups (Scheme 4) with 0.5 N HCl in THF yielded compound **28**. Hydrogenolysis of **28** with
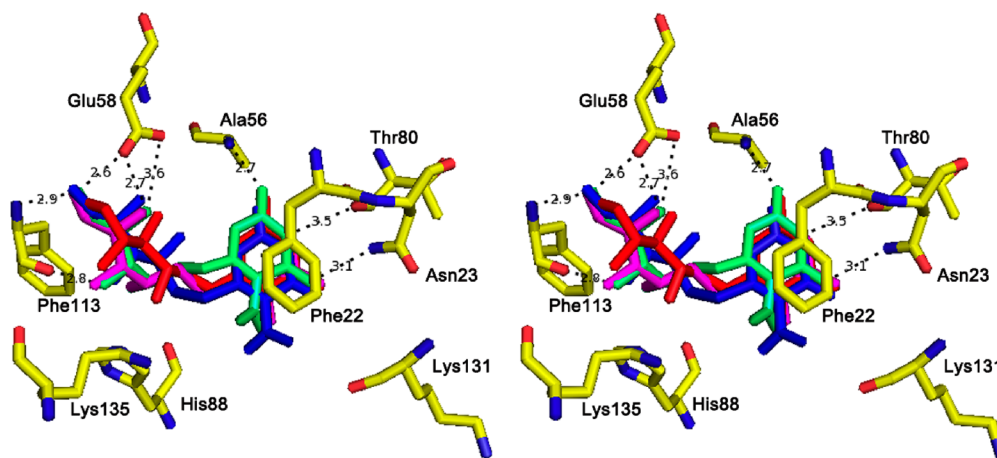

Figure 2. Calculated structures of the *O*- and *S*-nucleoside derivatives (**21**−**24**) complexed with *B. subtilis* lumazine synthase. The amino acid residues involved in the active site are labeled and shown as sticks. The black dashed lines represent the hydrogen bonds between one of the ligands and *B. subtilis* lumazine synthase. The color code for compound **21** is green, **22** is red, **23** is magenta, and **24** is blue. The maximum distance between the heavy atoms participating in the hydrogen bonds was set at 3.8 Å. This figure was generated by PyMol [DeLano, W. L. (2002), the PyMOL Molecular Graphics System, DeLano Scientific, San Carlos, CA, USA]. The figure is programmed for walleyed viewing.

Pd/C in MeOH containing 2 drops of HCl under atmospheric pressure afforded the desired *O*-nucleoside **29**.

Scheme 4
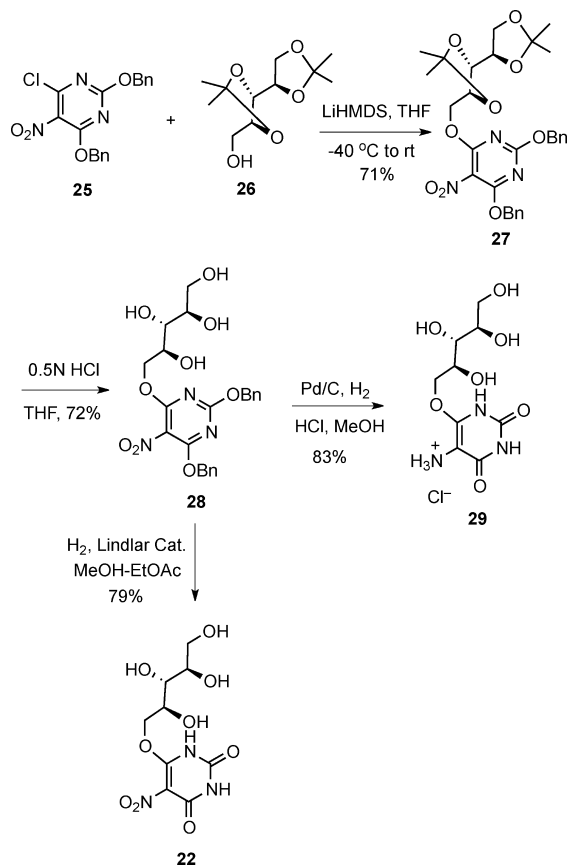
The next goal was to selectively remove the benzyl groups without reducing the nitro group. Lewis-acid-mediated cleavage of the benzyl groups proved to be futile. However, a hydrogenolysis reaction employing Lindlar catalyst provided solely compound **22** without even a trace of the amine **21** (Scheme 4).

Initially, dimethoxypyrimidine **31** was synthesized through a nucleophilic substitution reaction of **26** with 4-iodo-5-nitro-2,6-dimethoxypyrimidine (**30**) (Scheme 5).[46,47] The intended

Scheme 5
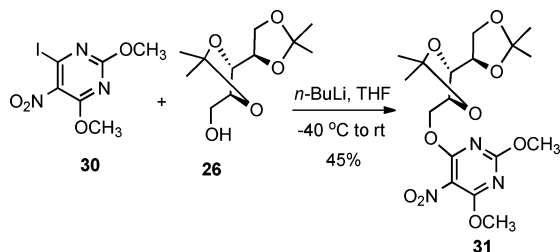
deprotection of the pyrimidinedione system at a relatively late stage in the synthesis under acidic or basic conditions was complicated by the fact that the ether linkage between the ribityl group and the pyrimidine ring was very labile. In most cases, the reaction gave rise to a mixture of products that were difficult to

isolate. This route was eventually abandoned in favor of the synthesis detailed in Scheme 4.

Compounds **36**, **40**, and **43** were chosen for synthesis because they are the oxygen analogues of the corresponding ribitylaminopyrimidines that were previously reported.[48] In order to provide a handle for the attachment of side chains at C-5 of the pyrimidine, the reduction of the nitro group in compound **27** was carried out in the presence of sodium hydrosulfite (Scheme 6) in refluxing 1,4-dioxane and methanol to provide amine **32**. The amine **32** was treated with ethyl chlorooxoacetate in the presence of Et₃N to afford ester **33**. Treatment of compound **33** with 0.5 N HCl in MeOH at room temperature proceeded to compounds **34** and **35** as a 1:1 mixture of methyl and ethyl esters. Compounds **34** and **35** were easily separated by flash column chromatography. Hydrogenolysis of compounds **34** in EtOH and **35** in MeOH in the presence of Pd/C provided the required products **36** and **37** in good yield. Compounds **40** and **43** were prepared by following a similar protocol. However, synthesis of **46** presented additional challenges because of the presence of the alkene in the side chain. Compound **46** is a bioisostere of an intermediate **6/17** involved in lumazine **3** biosynthesis. The amine **32** was treated with methacrolyl chloride to afford **44**. The double bond present on the side chain prevented application of the general hydrogenolysis protocol using Pd/C. Use of Lindlar catalyst (Scheme 4) was attempted, but unfortunately with compound **45** this led to both deprotection of the benzyl groups as well as reduction of double bond in the side chain to provide compound **40** instead of **46**. A modified protocol was devised in order to selectively remove the benzyl groups under controlled hydrogenolysis in which 1,4-cyclohexadiene was used as the source of hydrogen. Addition of 1,4-cyclohexadiene to a reaction mixture containing compound **45** and Lindlar catalyst gave rise to the desired pyrimidinedione **46**.

Synthesis of *S*-Nucleosides. The syntheses of *S*-nucleoside **23** and the nitro derivative **24** were described earlier.[49] The syntheses of additional metabolically stable sulfides that can structurally mimic the substrates, hypothetical intermediates, and products involved in 6,7-dimethyl-8-ribityllumazine (**3**) and riboflavin (**4**) biosynthesis were undertaken in order to explore the effects of sulfur incorporation. Following the standard protocol (Scheme 7), derivatization of the amine **47** with acid chlorides provided the expected amide products in very low yield. Reaction of **47** with various acids using peptide coupling synthesis methods was therefore explored. The reaction proceeded in only 10% yield in THF, but changing the solvent to pyridine increased the efficiency of the reaction so that moderate yields of **48** and **50** could be obtained. Removal of the acetonide protecting groups under acidic conditions afforded the desired sulfide derivatives **49** and **51**.

Synthesis of *N*-Nucleosides. The *N*-nucleosides **56**, **60**, **63**, **66**, and **69** were synthesized as metabolically stable analogues of the hypothetical intermediates **6**, **7**, **9**, and **10**. The synthesis of **56** started with a nucleophilic aromatic substitution reaction of compound **25** with ribitylamine to yield the expected product **52** (Scheme 8). TBDMS protection of the hydroxyl groups of the ribityl side chain was employed to avoid their reaction during acylation of the primary amino group attached to the pyrimidinedione ring in intermediate **54**. Compound **53**[50] was then reduced with sodium hydrosulfite to amine **54**. The amine **54** is very unstable and therefore it was not isolated. Acylation of the amine **54** with methacrolyl chloride afforded the amide **55**. Simultaneous removal of both types of protecting groups
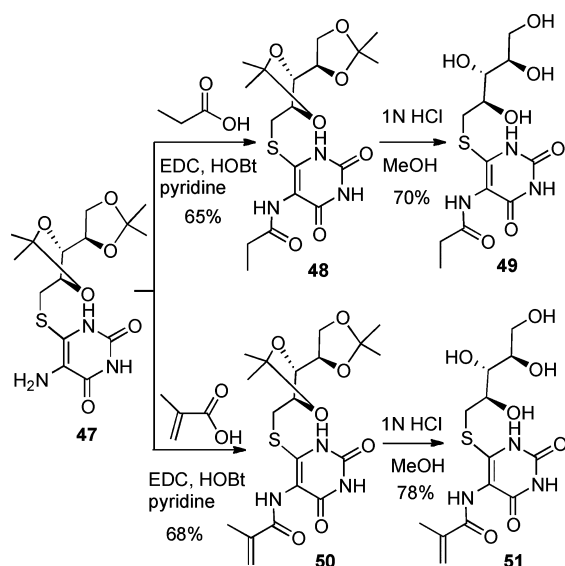
Scheme 6
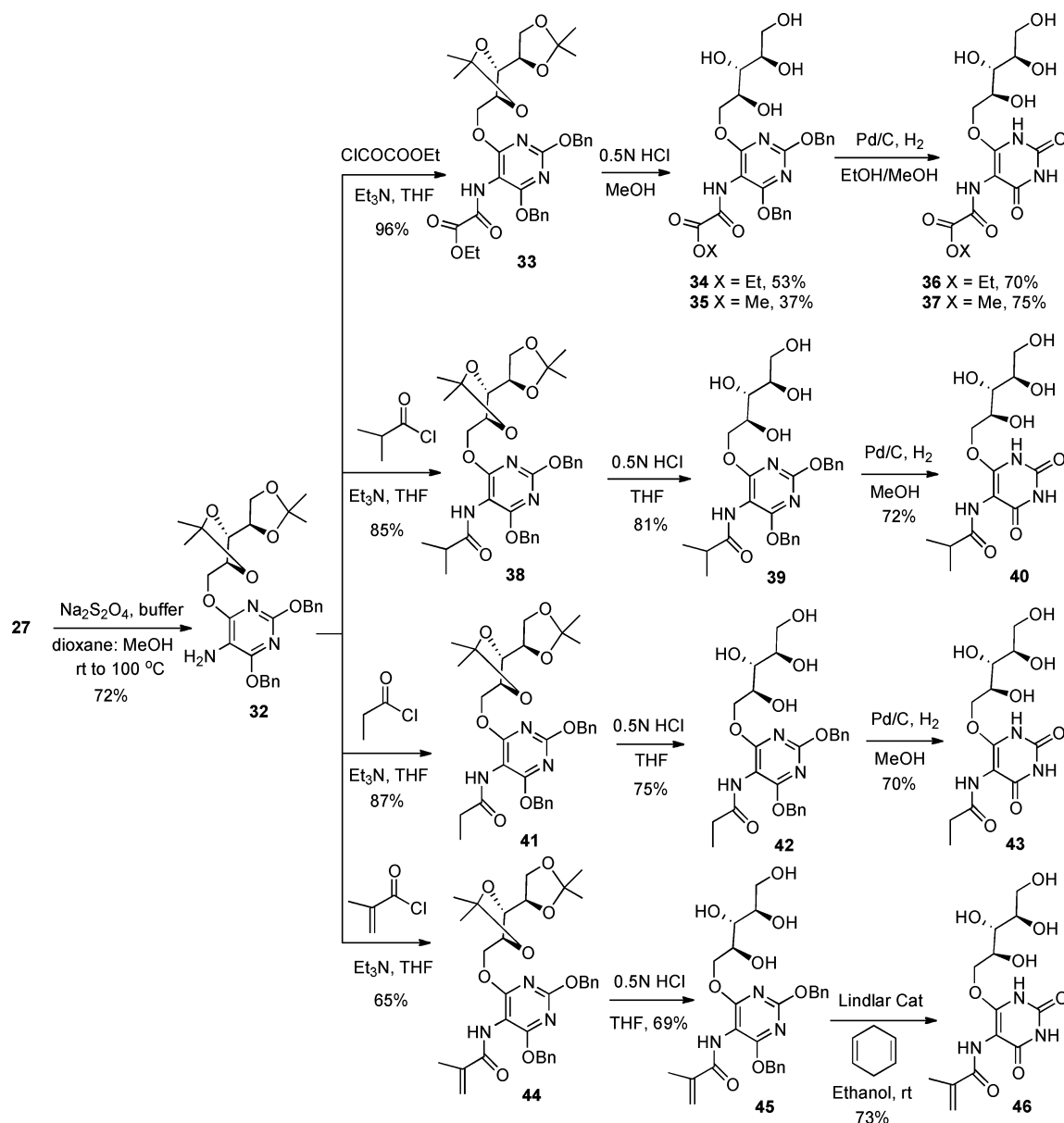
(TBDMS and methyl) was accomplished by heating intermediate **55** with HBr in aqueous methanol at 55−60 °C to afford the target compound **56**.

The synthesis outlined in Scheme 8 proceeded well except for the last step. Several alternate methods were tried to cleave the methyl groups, but none of them afforded the desired product. For example, heating at reflux in HCl/MeOH, reaction with Amberlite-IR-120 (H⁺)/MeOH, and stirring at room temperature with BBr₃/THF or TMSI/THF were all tried. The best method to cleave methyl groups in this case proved to be heating at reflux in HBr/MeOH solution. However, purification of the final product by flash chromatography (SiO₂) was difficult. Eluting with EtOAc/EtOH/H₂O/AcOH (67:23:9:1) was effective but leached silica gel from the column. Fortunately, the silica could be removed by passing compound **56** twice through Sephadex LH 20 columns.
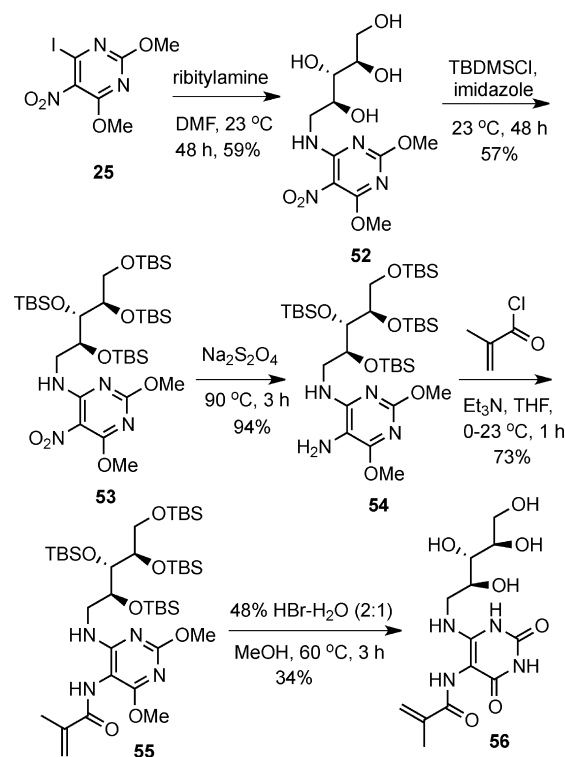
In order to avoid the problems faced during removal of the methyl groups, in subsequent syntheses, the protecting group was switched to benzyl. The unstable amine **57** was prepared

according to the reported procedure.[48] The amine **57** was reacted with 2-chloropropanoyl chloride, 2-chloroacetyl chloride, or 3,3,3-trifluoropropanoyl chloride to afford the corresponding amides **58**, **61**, and **64** (Scheme 9), which were deprotected with TBAF to yield **59**, **62**, and **65**. Removal of the benzyl protecting groups by catalytic hydrogenolysis using Lindlar or Pearlman's catalyst and 1,4-cyclohexadiene as a controlled source of hydrogen provided the desired products **60**, **63**, and **66**. The Lindlar catalyst worked fine for the conversion to compound **60**. Conversion of **62** to **63** and **65** to **66** using Lindlar catalyst was slow, but the hydrogenolysis reaction could be expedited by changing the catalyst to Pearlman's catalyst. For the synthesis of the compound **69** with a conformationally restricted side chain resembling the hypothetical carbinolamine intermediate **10**, 2-oxopropanoyl chloride was reacted with amine **57** in the presence of Et₃N at room temperature to afford intermediate **67**. The reagent 2-oxopropanoyl chloride was synthesized by reacting pyruvic acid with α,α-dichloromethyl methyl ether. Treatment of compound **67** with tetrabutylammo-

F

dx.doi.org/10.1021/jo3010364 | J. Org. Chem. XXXX, XXX, XXX−XXX

Scheme 7

47   **48**   **49**   **50**   **51**

EDC, HOBt pyridine 65%

1N HCl MeOH 70%

EDC, HOBt pyridine 68%

1N HCl MeOH 78%

Scheme 8

25   **52**   **53**   **54**   **55**   **56**

ribitylamine DMF, 23 °C 48 h, 59%

TBDMSCl, imidazole 23 °C, 48 h 57%

$Na_2S_2O_4$ 90 °C, 3 h 94%

Et_3N, THF, 0-23 °C, 1 h 73%

48% HBr-H_2O (2:1) MeOH, 60 °C, 3 h 34%

nium fluoride removed the TBDMS groups, and during the process, the intermediate underwent cyclization to yield **68**. Hydrogenolysis of **68** with Lindlar catalyst successfully provided the desired compound **69**.

The structures of some previously reported lumazine synthase and riboflavin synthase inhibitors are listed in Chart 3 for the purpose of comparison with the presently reported compounds.[41,42,48,51,52] The crystal structure of **75** bound to *M. tuberculosis* lumazine synthase (PDB code: 2C97)[41] encouraged the synthesis of compound **78**, which is described in Scheme 10.

Intermediate **80** was obtained by the reaction of **79**[52] with methacrolyl chloride. The chloride and double bond present in the intermediate **80** prevented the application of general

hydrogenolysis deprotection protocol using Pd/C. By applying our Lindlar catalyst/1,4-cyclohexadiene methodology, the benzylic groups were selectively removed under controlled hydrogenolysis conditions.

Lindlar Catalyst and Pearlman's Catalyst in Chemoselective Hydrogenolysis. The benzyl group is one of the most commonly used groups for the protection of oxygen and nitrogen functional groups in synthetic organic chemistry, as it is stable toward many reaction conditions and can be easily installed. Catalytic hydrogenolysis often offers the mildest method for removal of the benzyl ether protecting group. However, hydrogenolysis is often not compatible with the presence of other reducible functional groups, such as alkenes, nitro groups, and halogens. Several examples are provided here of the use of Lindlar catalyst, either with H_2 (compounds **22** and **69**) or with 1,4-cyclohexadiene (compounds **46**, **60**, and **78**), as the source of hydrogen. Pearlman's catalyst was successful with 1,4-cyclohexadiene as the source of hydrogen in the cases of compounds **63** and **66**.

Enzyme Inhibition Studies. The lumazine synthase substrate analogues and hypothetical intermediate analogues were tested as inhibitors of the recombinant lumazine synthases of *Bacillus subtilis*, *Mycobacterium tuberculosis*, and *Schizosaccharomyces pombe*, as well as the recombinant riboflavin synthase of *Escherichia coli* and *Mycobacterium tuberculosis*. The inhibition constants and inhibition mechanisms of these inhibitors are listed in Table 1 along with the previously reported compounds **70**–**77**, which are also included in Table 1 for comparison. All of the synthesized metabolically stable oxalamic acid derivatives with S, O, and NH linkages between the ribityl side chain and pyrimidinedione ring are analogues of the phosphate elimination intermediate **6** of the lumazine synthase-catalyzed reaction. Except for compound **72**,[48] these probes without a phosphate side chain were in general found to be moderately active or inactive lumazine synthase inhibitors. However, some of the new compounds did display submicromolar K_i values versus some of the enzyme. These include **23** versus *S. pombe* lumazine synthase, **24** versus *M. tuberculosis* riboflavin synthase, and **69** versus *M. tuberculosis* riboflavin synthase. Compound **72** was found to be an outlier with unusually high inhibitory potency versus *E. coli* riboflavin synthase (K_i 0.0013 μM).

The relative efficacies of the *N*-nucleoside, *O*-nucleoside, *S*-nucleoside, and *C*-nucleoside substrate analogue inhibitors can be directly accessed by comparison of the nitro compounds **18** (Figure 1) (K_i 13 μM[49]), **22** (K_i 60 μM, Table 1), **24** (K_i 11 μM[49]), and **73** (K_i 220 μM[49]) versus *M. tuberculosis* lumazine synthase. The *S*-nucleosides were generally more potent than the corresponding *O*-nucleosides, as exemplified by the relative activities of the *S*-nucleosides **49** (K_i 128 μM) and **51** (K_i 198 μM) versus the *O*-nucleosides **43** (K_i >1000 μM) and **46** (K_i >1000 μM) against *M. tuberculosis* lumazine synthase. The *S*-nucleoside **23**[49] having an amino group at C-5 of the pyrimidinedione was found to be a relatively potent inhibitor of the lumazine synthases of *S. pombe* (K_i 0.16 μM), *B. subtilis* (K_i 2.6 μM), and *M. tuberculosis* (K_i 31 μM) and of the riboflavin synthases of *M. tuberculosis* (K_i 2.5 μM) and *E. coli* (K_i 47 μM), whereas the *C*-nucleoside analogue **74**[51] of the substrate **1** was shown previously to be completely inactive against *B. subtilis* lumazine synthase.[51]

Compound **75**[41] displayed a K_d of 0.72 μM versus *M. tuberculosis* lumazine synthase. Compounds **76**,[52] **77**,[52] and **78** had very weak or no enzyme inhibitory activity. Although compound **75** lacks the ribityl side chain, it has a phosphate
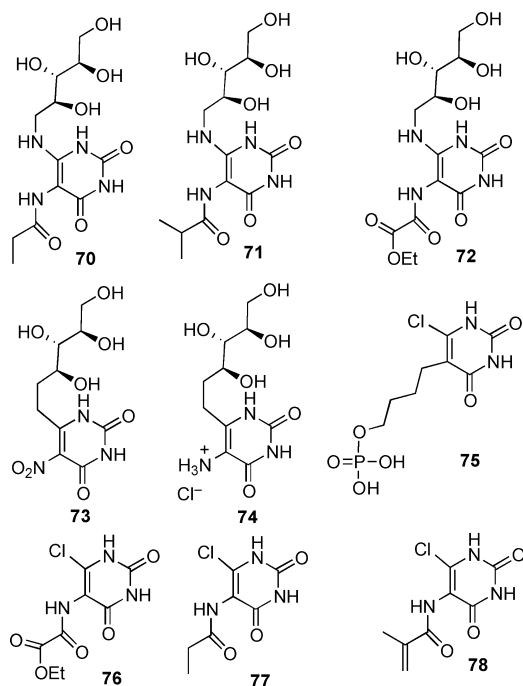
Scheme 9
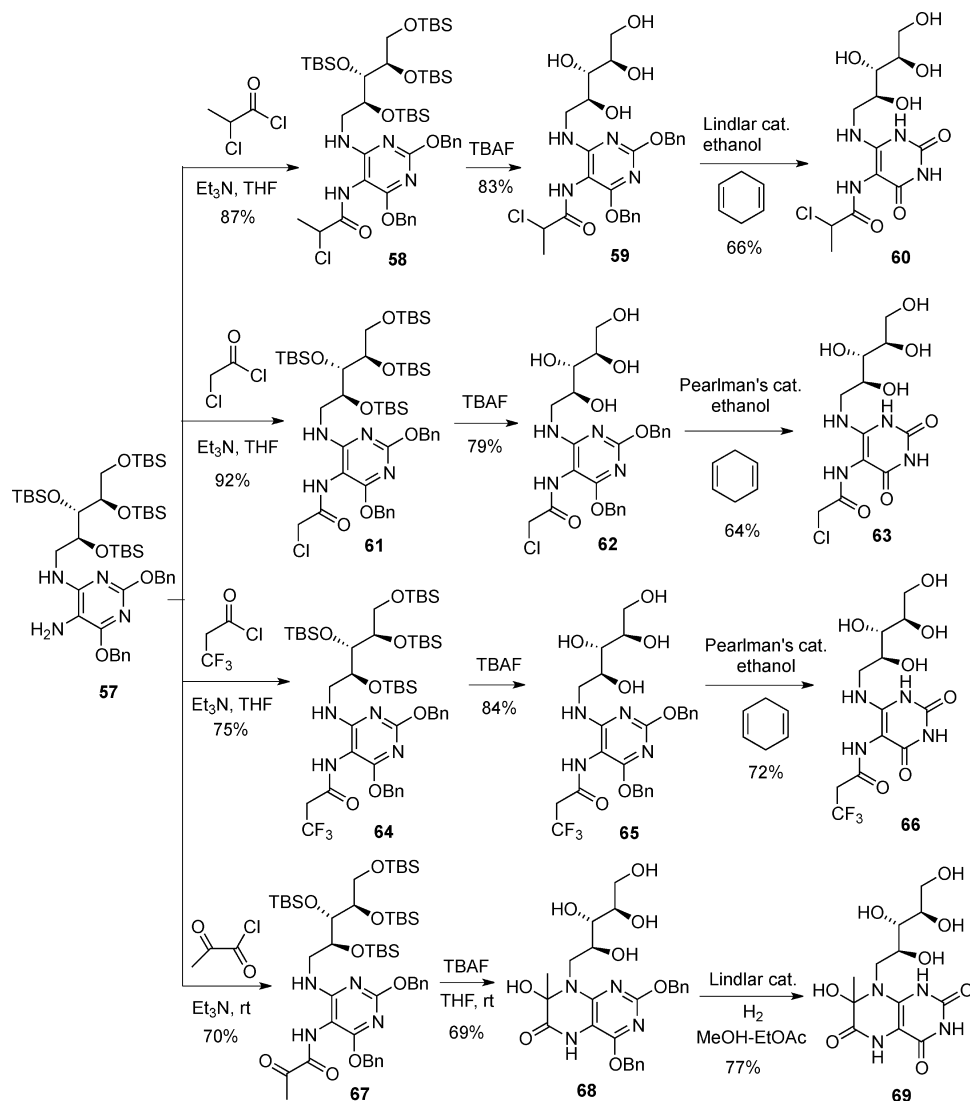
moiety that contributes positively to binding. The inhibitory activity is probably due in large part to the presence of the phosphate group that binds in the phosphate binding pocket of the enzyme.[41] It also has a $\pi-\pi$ stacking interaction of the pyrimidinedione ring with Trp27.

The N-nucleoside ethyl oxalate derivative 72[48] proved to be an unusually potent inhibitor of $E.\ coli$ riboflavin synthase, with a K_i of 0.0013 μM. It also had a K_i of 4.0 μM against $M.\ tuberculosis$ lumazine synthase, whereas the O-nucleoside ethyl oxalate derivative 36 is completely inactive against all lumazine synthases and riboflavin synthases tested. In contrast, the methyl oxalate derivative 37 had weak activity (K_i of 868 μM) against $M.\ tuberculosis$ riboflavin synthase. The potency and the structure of the compound 72 are reminiscent of the potent 6,7-dihydro-6,7-dioxo-8-ribityllumazine system 81 (Chart 4), which was previously shown to be a potent inhibitor of baker's yeast riboflavin synthase (K_i 0.025 μM) and $Ashbya\ gossypii$ riboflavin synthase (K_i 0.009 μM).[53,54] It should be noted, however, that 72 (K_i 0.0013 μM) is more potent versus $E.\ coli$ riboflavin synthase than 81 (K_i 0.0062 μM) by a factor of 4.8. In this particular case, the greater flexibility of 72 versus 81 may allow it to better fit the binding pocket of the enzyme. The previously synthesized, conformationally restricted compound 84 was also found to be a

less potent inhibitor (K_i 0.61 μM) of $E.\ coli$ riboflavin synthase.[55] It is possible that the dioxolumazine 81 is a more potent riboflavin synthase inhibitor than 84 because it resembles the hypothetical intermediate 11 involved in the reaction catalyzed by riboflavin synthase.[56] The related compound 69 is also a relatively potent inhibitor of $M.\ tuberculosis$ riboflavin synthase (K_I 0.74 μM), although it is not nearly as potent as the dioxo compound 81. Compound 69, which resembles intermediate 10 in the lumazine synthase-catalyzed reaction, inhibits $M.\ tuberculosis$ lumazine synthase with a K_i value of 8.6 μM.

The O-nucleosides 36, 40, and 43 were synthesized as the oxygen analogues of the N-nucleoside inhibitors 72 (K_i 4 μM), 71 (K_i 42 μM), and 70 (K_i 110 μM) of $M.\ tuberculosis$ lumazine synthase. In contrast to the N-nucleoside inhibitors, the O-nucleosides 36, 40, and 43 were totally inactive versus lumazine synthase. The N-nucleoside 70 had a K_i of 110 μM versus $M.\ tuberculosis$ lumazine synthase, while the corresponding S-nucleoside 49 had a K_{is} of 128 μM versus $M.\ tuberculosis$ lumazine synthase. Crystallographic studies of 70 bound to $M.\ tuberculosis$ lumazine synthase have revealed a water bridge between the ribitylamino NH and the side chain amino group of Lys138 (PDB code: 2VI5).[48] The greater activity of the N-nucleosides may reflect the ability of the ribitylamino NH to

H

dx.doi.org/10.1021/jo3010364 | J. Org. Chem. XXXX, XXX, XXX−XXX

Chart 3

Scheme 10
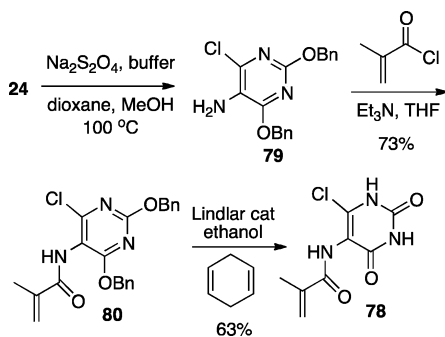
function as a hydrogen bond donor toward the bridging water molecule, in contrast to the *C*-, *O*-, and *S*-nucleosides, which cannot act as hydrogen bond donors. It seems less likely that the NH of the ribitylamino group could act as a hydrogen bond acceptor because it is part of a vinylogous amide system. A related set of compounds that allows comparison is the *S*-nucleoside **49** (K_i 128 μM), the *N*-nucleoside **70** (K_i 110 μM), and the *O*-nucleoside **43** (inactive). The one *N*-nucleoside that does not fit the pattern at all is **56**, which proved to be inactive versus *M. tuberculosis* lumazine synthase.

With regard to the new monocyclic lumazine synthase intermediate analogues, whose syntheses are outlined in Scheme 8 and Scheme 9, the activity order versus *M. tuberculosis* lumazine synthase is **63** (K_i 57 μM) > **66** (K_i 100 μM) > **60** (K_i 279 μM) > **56** (K_i > 1000 μM). In the case of *E. coli* riboflavin synthase, the order is reversed: **56** (K_i 52 μM) > **60** (K_i 314 μM) > **66** (K_i > 1000 μM) = **63** (K_i > 1000 μM). The bicyclic compound **69** is exceptional because it is the most active of the new compounds versus both *M. tuberculosis* lumazine synthase (K_i 8.6 μM) and *E. coli* riboflavin synthase (K_i 0.74 μM). However, none of the compounds in this series can match the potency versus *M. tuberculosis* lumazine synthase displayed by compounds with phosphate side chains (e.g., **85**, K_i 0.0041 μM).[37]

MD Simulation and Binding Energy Calculations. Although the mechanism probes **36** and **72** differ only in the heteroatom linkage between the ribityl side chain and the pyrimidinedione ring, they have a very large difference in their inhibitory activities against *M. tuberculosis* lumazine synthase and *E. coli* riboflavin synthase. In compounds **69** and **81**, the C-5 side chains of **82** and **72** have been conformationally restricted through cyclization and they have shown good inhibitory activities against *M. tuberculosis* lumazine synthase and *M. tuberculosis* riboflavin synthase (Chart 4). In the case of lumazine synthase, conformational restriction of the side chain appears to increase the inhibitory activity. To understand these results, a series of molecular dynamics simulations followed by free energy calculations using the Poisson−Boltzmann/surface area (MM-PBSA) method were carried out.[57] All simulations were performed using AMBER 9.0. For each ligand, the force field parameters were taken from the general Amber force field (GAFF), whereas the atomic partial charges were derived by geometry optimization using the Gaussian 03 package.[58] These analyses have suggested a molecular basis for the interaction of these compounds with lumazine synthase, and they have provided a practical method to predict ligand binding affinities in future applications.

MD Simulations of the *M. tuberculosis* Lumazine Synthase Complex with Ligand 70. The X-ray crystal structure of ligand **70** and *M. tuberculosis* lumazine synthase complex is available from the Protein Data Bank (PDB code: 2VI5).[48] The C-5 sp^2 carbon of the ligand in this structure appears distorted and deviates from its standard geometry, and therefore the starting structure was thoroughly energy minimized to ensure the right ligand conformation before MD simulation. The whole simulation time was 1000 ps, during which the ligand remained stable in the binding site and the ligand rmsd remain at about 0.7 Å (in Figure 3, black). Hydrogen bond analysis revealed that most of the hydrogen bonds and water bridges that are apparent in the crystal structure were retained during the simulation.

MD Simulations of the *M. tuberculosis* Lumazine Synthase Complex with Ligand 81. Ligand **81** binds tightly to the active site of *M. tuberculosis* lumazine synthase during the entire MD simulation process. As shown in Figure 3 (red), the ligand rmsd remained quite small, around 0.2−0.3 Å, during the whole simulation time. Figure 4 shows the minimized average structure of the binding site of lumazine synthase complex with ligand **81**. Compared to ligand **70**, the additional ring system in ligand **81** did not result in much change in the overall binding mode, and most of the hydrogen bonds to the binding site residues (including Ala59, Ile60, Glu61, Val81, and Asn114) were retained with ligand **81**, as well as the two water bridges. The most remarkable difference was the formation of two hydrogen bonds with Lys138 and Gln141, which were not observed with ligand **70**. As shown in Figure 5 (top), the hydrogen bond between the diketone carbonyl oxygen (O-7) and NH$_2$ of Gln141 formed at 400 ps in the MD simulation when the side chain of Gln141 rotated 90° to approach the carbonyl group (O-7) of ligand **81**. The distance between the (O-7) carbonyl oxygen on ligand **81** and the NH$_2$ side chain hydrogen of Gln141 fluctuates around 1.95 Å during the next 600 ps of the MD simulation, indicating a tight hydrogen bond between them. The MD simulation also revealed a stable hydrogen bond between the NH$_2$ of Lys138 and the (O-6) carbonyl oxygen of ligand **81**. The three hydrogens on the protonated amino group of Lys138 are constantly rotating and form a hydrogen bond with

Table 1. Inhibition Constants versus *S. pombe* Lumazine Synthase, *M. tuberculosis* Lumazine Synthase, *B. subtilis* Lumazine Synthase, *M. tuberculosis* Riboflavin Synthase, and *E. coli* Riboflavin Synthase
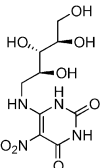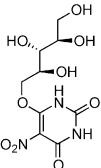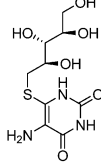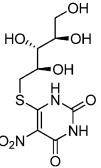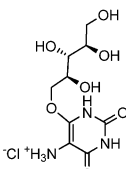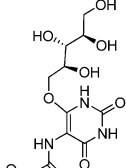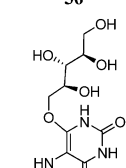
Compd	Enzyme	K_s,[e] μM	K_{cat},[f] m^{-1}	K_i,[g] μM	K_{is},[h] μM	Mechanism
18	*B. subtilis* LS[a]	12 ± 2	1.2 ± 0.1	16 ± 1		Competitive
	M. tuberculosis LS	52 ± 6	0.12 ± 0.01	13 ± 1		Competitive
	E. coli RS[b]	2.6 ± 0.3	8.7 ± 0.2	8.0 ± 1.9	65 ± 19	Mixed
	M. tuberculosis RS[c]	18 ± 2	0.40 ± 0.02	4.2 ± 0.3		Competitive
22	*S. pombe* LS[b]	1.4 ± 0.1	1.4 ± 0.0	55 ± 14	110 ± 40	Partial
	M. tuberculosis LS[d]	25 ± 2	0.19 ± 0.00	60 ± 5		Competitive
	E. coli RS	2.6 ± 0.2	3.3 ± 0.01	38 ± 3		Competitive
	M. tuberculosis RS	7.1 ± 0.7	0.26 ± 0.01	36 ± 15	26 ± 6	Partial
23	*B. subtilis* LS	16 ± 2	1.1 ± 0.1	2.6 ± 0.2		Competitive
	S. pombe LS	0.59 ± 0.06	1.7 ± 0.0	0.16 ± 0.01		Competitive
	M. tuberculosis LS[c]	30 ± 4	0.19 ± 0.01	31 ± 11	57 ± 24	Partial
	E. coli RS	5.7 ± 0.5	4.0 ± 0.2	47 ± 14	122 ± 52	Partial
	M. tuberculosis RS	4.9 ± 0.3	0.25 ± 0.01	2.5 ± 0.1		Competitive
24	*B. subtilis* LS	21 ± 3	1.3 ± 0.1	26 ± 3		Competitive
	S. pombe LS	2.3 ± 0.2	5.1 ± 0.1	2.0 ± 0.2		Competitive
	M. tuberculosis LS	36 ± 3	0.20 ± 0.01	11 ± 2	62 ± 23	Mixed
	E. coli RS	2.8 ± 0.2	4.8 ± 0.1	2.7 ± 0.4	32 ± 8	Partial
	M. tuberculosis RS	2.8 ± 0.2	0.18 ± 0.00	0.56 ± 0.14	4.7 ± 1.8	Partial
29	*S. pombe* LS	1.2 ± 0.1	1.3 ± 0.0	14 ± 3	43 ± 8	Partial
	M. tuberculosis LS	27 ± 2	0.18 ± 0.01		>1000	Uncompetitive
	E. coli RS	2.5 ± 0.1	3.2 ± 0.1		>1000	Uncompetitive
	M. tuberculosis RS	5.6 ± 0.5	0.25 ± 0.01		577 ± 121	Uncompetitive
36	*S. pombe* LS	6.4 ± 0.6	2.7 ± 0.1		>1000	Uncompetitive
	M. tuberculosis LS	34 ± 5	0.26 ± 0.01		>1000	Uncompetitive
	E. coli RS	3.0 ± 0.3	5.8 ± 0.2		>1000	Uncompetitive
	M. tuberculosis RS	5.0 ± 0.5	0.25 ± 0.01		>1000	Uncompetitive
37	*S. pombe* LS	1.7 ± 0.2	1.5 ± 0.0	43 ± 15	56 ± 15	Partial
	M. tuberculosis LS	29 ± 2	0.18 ± 0.00	273 ± 55		Competitive
	E. coli RS	3.1 ± 0.2	3.4 ± 0.1		>1000	Uncompetitive
	M. tuberculosis RS	4.1 ± 0.4	0.22 ± 0.01		868 ± 305	Uncompetitive

Table 1. continued
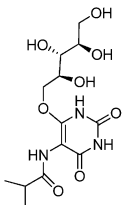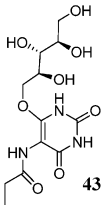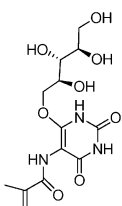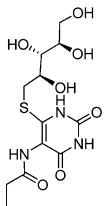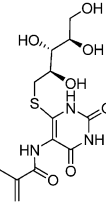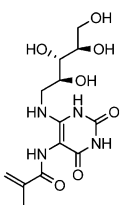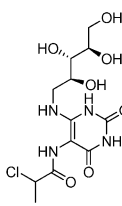
Compd	Enzyme	K_s,[e] μM[e]	K_{cat},[f] m^{-1}	K_i,[g] μM	K_{is},[h] μM	Mechanism
40	*M. tuberculosis* LS	16 ± 1	0.59 ± 0.01		766 ± 97	Uncompetitive
	M. tuberculosis RS	9.3 ± 0.6	0.84 ± 0.02		698 ± 108	Uncompetitive
43	*M. tuberculosis* LS	18 ± 2	0.39 ± 0.00		1000	Uncompetitive
	M. tuberculosis RS	4.4 ± 0.2	0.21 ± 0.00		>1000	Uncompetitive
46	*M. tuberculosis* LS	12 ± 1	0.57 ± 0.01		>1000	Uncompetitive
	M. tuberculosis RS	9.2 ± 0.6	0.58 ± 0.01		>1000	Uncompetitive
49	*M. tuberculosis* LS	11 ± 1	0.65 ± 0.01	128 ± 31		Competitive
	M. tuberculosis RS	10 ± 1	0.76 ± 0.01		> 1000	Uncompetitive
51	*M. tuberculosis* LS	17 ± 1	0.92 ± 0.03	198 ± 72		Competitive
	M. tuberculosis RS	10 ± 0	0.84 ± 0.01		> 1000	Uncompetitive
56	*M. tuberculosis* LS	19 ± 2	0.52 ± 0.02		> 1000	Uncompetitive
	M. tuberculosis RS	7.0 ± 0.6	0.57 ± 0.02	52 ± 22	35 ± 14	Partial
60	*M. tuberculosis* LS	17 ± 1	0.85 ± 0.03	279 ± 112		Competitive
	M. tuberculosis RS	11 ± 1	0.72 ± 0.01	314 ± 49		Competitive

Table 1. continued
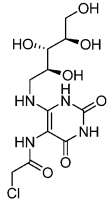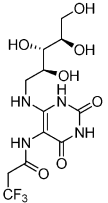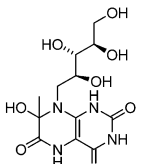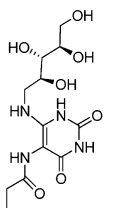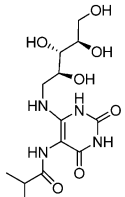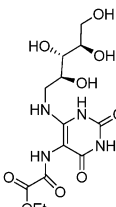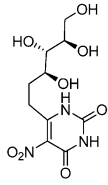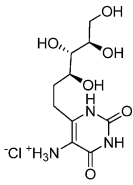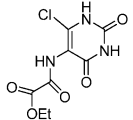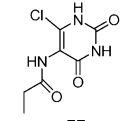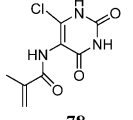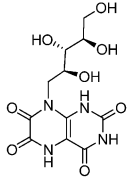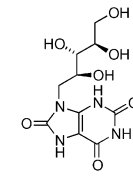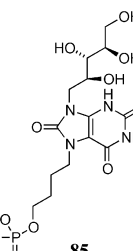
Compd	Enzyme	K_s,[e] μM^e	K_{cat},[f] m^{-1}	K_i,[g] μM	K_{is},[h] μM	Mechanism
63	*M. tuberculosis* LS	24 ± 2	0.62 ± 0.02	57 ± 22	53 ± 12	Partial
	M. tuberculosis RS	8.6 ± 0.4	0.66 ± 0.01		> 1000	Uncompetitive
66	*M. tuberculosis* LS	20 ± 1	0.76 ± 0.02	100 ± 20	309 ± 125	Partial
	M. tuberculosis RS	6.6 ± 0.3	0.18 ± 0.1		> 1000	Uncompetitive
69	*M. tuberculosis* LS	19 ± 2	0.59 ± 0.02	8.6 ± 0.7		Competitive
	M. tuberculosis RS	8.9 ± 0.7	0.67 ± 0.02	0.74 ± 0.05		Competitive
70	*B. subtilis* LS	3.2 ± 0.3	0.37 ± 0.01	20 ± 4	56 ± 12	Partial
	M. tuberculosis LS	58 ± 8	0.095 ± 0.005	110 ± 14		Competitive
	S. pombe LS	1.9 ± 0.3	1.3 ± 0.1	11 ± 1		Competitive
	E. coli RS	6.3 ± 0.7	12 ± 0		>1000	Uncompetitive
71	*B. subtilis* LS	3.6 ± 0.3	0.40 ± 0.01	95 ± 36	64 ± 11	Partial
	M. tuberculosis LS	63 ± 8	0.11 ± 0.01	42 ± 16	77 ± 28	Partial
	S. pombe LS	1.1 ± 0.1	0.95 ± 0.02	7.9 ± 0.8		Competitive
	E. coli RS	5.9 ± 0.6	12 ± 1		>1000	Uncompetitive
72	*B. subtilis* LS	5.4 ± 0.5	2.5 ± 0.1	607 ± 177		Competitive
	M. tuberculosis LS	53 ± 11	0.11 ± 0.01	4.0 ± 1.7	35 ± 14	Partial
	S. pombe LS	1.0 ± 0.1	10 ± 0.0	1.1 ± 0.2	15 ± 3	Mixed
	E. coli RS	2.6 ± 0.2	16 ± 0	0.0013 ± 0.0001	0.34 ± 0.08	Mixed
73	*B. subtilis* LS	14 ± 1	1.0 ± 0.0	309 ± 52		Competitive
	E. coli RS	2.0 ± 0.2	5.5 ± 0.1	37 ± 5	860 ± 270	Partial
	M. tuberculosis RS	20 ± 2	0.36 ± 0.02	8.4 ± 0.6		Competitive

Table 1. continued

Compd	Enzyme	K_s,[e] μM[e]	K_{cat},[f] m^{-1}	K_i,[g] μM	K_{is},[h] μM	Mechanism
74	*B. subtilis* LS	14 ± 1	1.0 ± 0.1		> 1000	Uncompetitive
	M. tuberculosis LS	58 ± 5	0.19 ± 0.01	357 ± 63		Competitive
	E. coli RS	2.4 ± 0.2	8.4 ± 0.1		> 1000	Uncompetitive
	M. tuberculosis RS[c]	22 ± 3	0.38 ± 0.02		>1000	Uncompetitive
76	*M. tuberculosis* LS	21 ± 2	0.61 ± 0.02		> 1000	Uncompetitive
	M. tuberculosis RS	7.8 ± 0.3	0.34 ± 0.01		897 ± 104	Uncompetitive
77	*M. tuberculosis* LS	20 ± 1	0.58 ± 2		> 1000	Uncompetitive
	M. tuberculosis RS	9.4 ± 0.5	0.43 ± 0.03		>1000	Uncompetitive
78	*M. tuberculosis* LS	18 ± 2	0.53 ± 0.03		>1000	Uncompetitive
	M. tuberculosis RS	8.6 ± 0.4	0.58 ± 0.4		694 ± 88	Uncompetitive
81	*B. subtilis* LS	6.3 ± 0.5	2.6 ± 0.1	7.8 ± 0.5		Competitive
	M. tuberculosis LS	25 ± 4	1.1 ± 0.1	1.4 ± 0.1		Competitive
	E. coli RS	2.7 ± 0.2	15 ± 0	0.0062 ± 0.0005		Competitive
84	*B. subtilis* LS	2.2 ± 0.3	1.9 ± 0.1	46 ± 5	250 ± 42	Partial
	M. tuberculosis LS	27 ± 5	0.54 ± 0.02	9.1 ± 0.6		Competitive
	E. coli RS	9.6 ± 0.9	39.9 ± 0.7	0.61 ± 0.05		Competitive
85	*M. tuberculosis* RS	63 ± 6	1.4 ± 0.1	0.0041 ± 0.0023		Competitive
	E. coli RS	2.1 ± 0.2	17 ± 0	332 ± 83		Competitive

[a]Recombinant β_{60} capsid from *B. subtilis*. [b]Recombinant riboflavin synthase from *E. coli*. [c]Recombinant homopentameric lumazine synthase from *S. pombe*. [e]Recombinant riboflavin synthase from *M. tuberculosis*. [d]Recombinant homopentameric lumazine synthase from *M. tuberculosis*. The assays with lumazine synthase were performed with substrate **2** held constant, while the concentration of the pyrimidinedione substrate **1** was varied. [i]K_s is the substrate dissociation constant for the equilibrium E + S ⇌ ES. [f]K_{cat} is the rate constant for the process ES → E + P. [g]K_i is the inhibitor dissociation constant for the process E + I ⇌ EI. [h]K_{is} is the inhibitor dissociation constant for the process ES + I ⇌ ESI. The reaction mixtures contained 50 mM Tris·HCl, pH 7.0.

the (O-6) carbonyl oxygen of ligand **81** alternately during the entire simulation time, as shown in Figure 5 (bottom).

According to Table 2, the estimated binding free energy (using MM-PBSA method) for ligand **81** is −42.93 kJ/mol, much lower than ligand **70** (−30.98 kJ/mol), which is consistent with the results of the experimental enzyme inhibition assay. The enhanced affinity of ligand **81** could be attributed to the following three factors. First, there is the addition of two

Chart 4
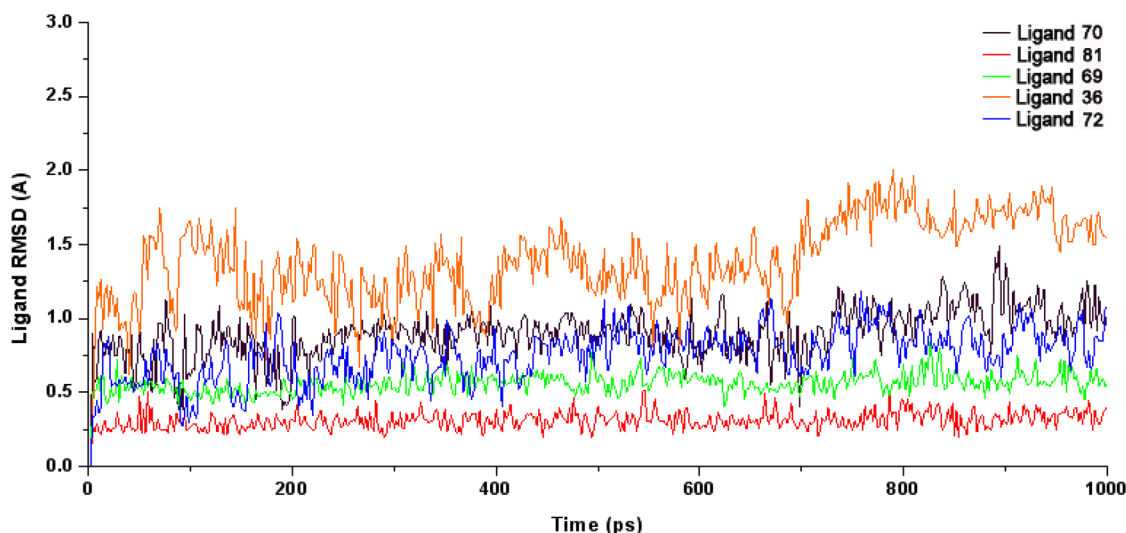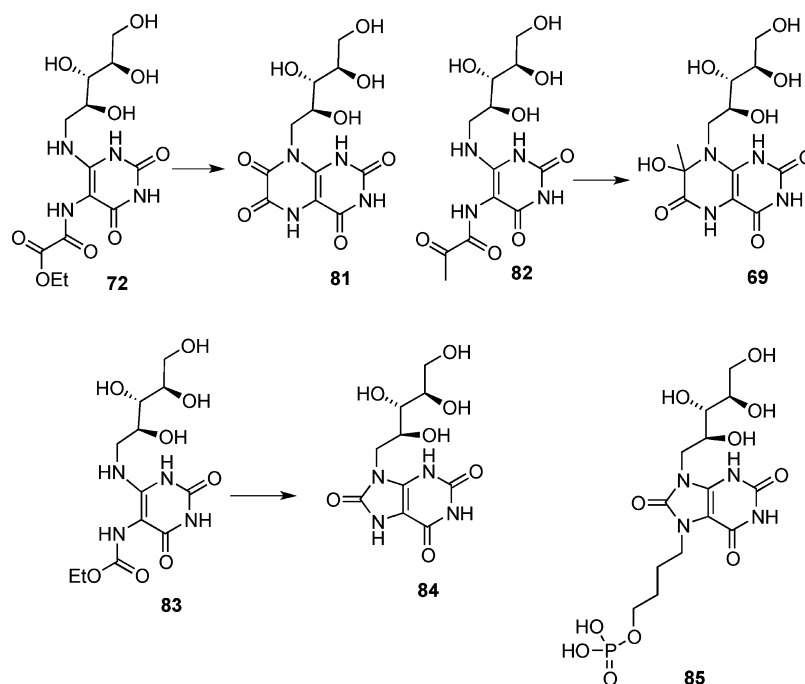
Figure 3. Time-dependent rmsd profile of the ligands in molecular dynamics simulations.

hydrogen bonds with Lys138 and Gln141. Evidence comes from the analysis of the electrostatic (ΔE_{elec}) term contribution to the binding free energy in Table 2. The electrostatic term in ligand **81** (−78.45 kJ/mol) is much lower than that in **70** (−63.10 kJ/mol), which dominates their difference in binding free energy. Second, because of the introduction of the additional dioxolumazine ring system, the π−π interaction with Trp27 is expected to be strengthened in ligand **81**. In Table 2, the van der Waals term (ΔE_{vdw}) of ligand **81** (−38.09 kJ/mol) is quite close to that of ligand **70** (−39.67 kJ/mol). In ligand **70**, the amide side chain protrudes into a hydrophobic pocket around Phe90 and Val93, and these hydrophobic interactions are largely compensated by the enhanced π−π interaction with Trp27 in ligand **81**. Third, the enhanced binding of ligand **81** in the active site of lumazine synthase can be attributed to the change in entropy. The 1,2-diketone chain is conformationally restricted in ligand

81, which would decrease the entropy loss during binding to the lumazine synthase binding site. Although the entropy loss is not explicitly estimated in this paper because of the tremendous calculation needed, it is an important factor.

MD Simulations of the *M. tuberculosis* Lumazine Synthase Complex with Ligand 69. Ligand **69** is also calculated to bind tightly in the binding site. The ligand rmsd stays at 0.5 Å (Figure 3, green). Ligand **69** can also form a hydrogen bond between the carbonyl oxygen (O-6) with NH_2 of Lys138, but not with Gln141. The estimated binding free energy for ligand **69** is −35.87 kJ/mol, which is a bit higher than that of ligand **81**. The difference mostly originates from the high desolvation energy (ΔG_{solv}) for ligand **69** (88.74 kJ/mol compared to 73.61 kJ/mol for ligand **81**). Since a hydroxyl group is more polar than a carbonyl group and can act as a hydrogen bond donor as well as a hydrogen bond acceptor, the
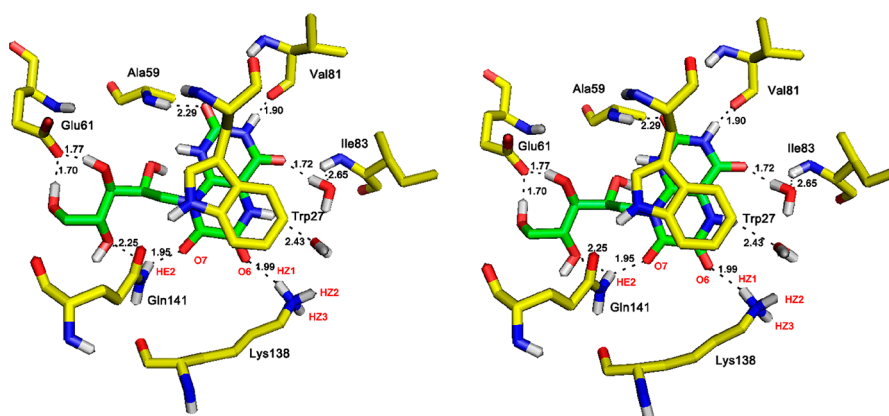
Figure 4. Molecular interactions between ligand **81** and *M. tuberculosis* lumazine synthase. Residues of the enzyme are labeled and shown as sticks. Hydrogen bonding interactions are indicated by black dashed lines with key distance. The figure is programmed for walleyed viewing.
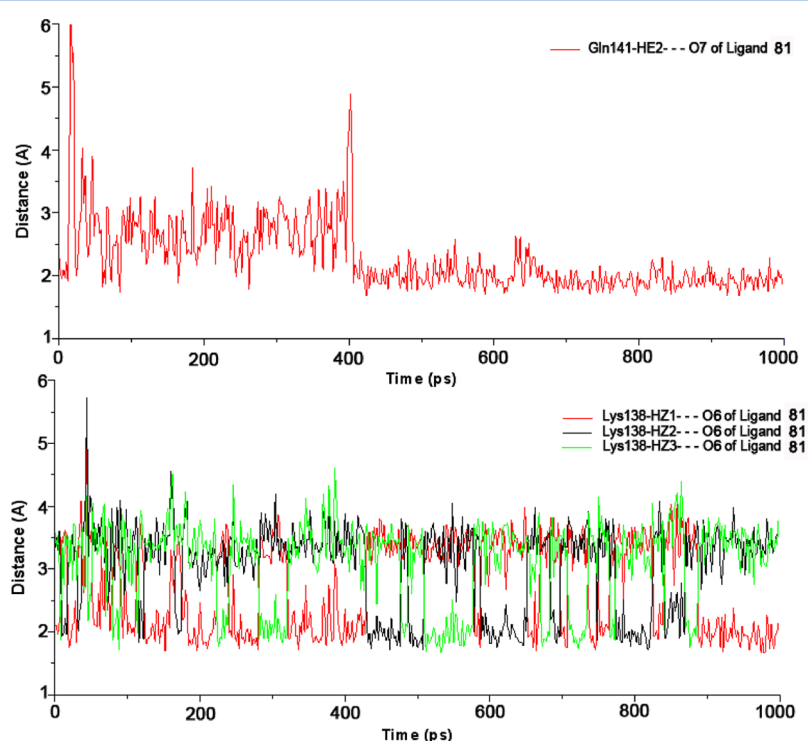
Figure 5. Time dependence of the key distances for the complex of ligand **81** with lumazine synthase during molecular dynamics simulations.

Table 2. Energy Contributions to Free Energy of Binding Calculated for Each Compound with the *M. tuberculosis* Lumazine Synthase Complex[a]

compd	ΔE_{elec}	ΔE_{vdw}	ΔG_{solv}	ΔG_{bind}	K_i (μM)
36	−59.18	−42.80	80.57	−21.41	>1000
69	−86.93	−37.69	88.74	−35.87	8.6 ± 0.7
70	−63.10	−39.67	71.78	−30.98	110 ± 14
72	−65.25	−44.24	83.64	−25.84	4.0 ± 1.7
81	−78.45	−38.09	73.61	−42.93	1.4 ± 0.1

[a]All energies are expressed as kJ/mol.

polar C-7 hydroxyl group makes ligand **69** more hydrophilic than ligand **81** and elevates its desolvation energy.

MD Simulations of the *M. tuberculosis* Lumazine Synthase Complex with Ligands 36 and 72. Ligand **36** is inactive in the experimental inhibitory activity assay. Consistent with this result, ligand **36** appears to be very unstable during the

entire MD simulation. The ligand rmsd fluctuates mainly between 0.7 and 1.7 Å, with the highest rmsd up to 2 Å (in Figure 3, orange). The instability comes from the steric clash between the long 1,2-dicarbonyl side chain and the lumazine synthase binding pocket. As a result, the estimated binding free energy for ligand **36** is −21.41 kJ/mol, which is much higher than that of ligands **69**, **72**, and **81**. The estimated binding free energy for ligand **36** is consistent with poor binding.

Ligands **36** and **72** differ only in the heteroatom linkage. Consequently, the dynamic behavior of ligand **72** is nearly the same as ligand **36** in the MD simulations. The ligand **72** also experiences large fluctuations during simulation. The ligand rmsd fluctuates between 0.5 and 1.0 Å (in Figure 3, blue). The binding free energy calculated for ligand **72** is only −25.84 kJ/mol, which is not consistent with its inhibitory activity relative to the other ligands in Table 2.

CONCLUSION

In conclusion, this article describes a comprehensive study of *O*-nucleoside, *S*-nucleoside, and *N*-nucleoside probes that has provided insights into the mechanistic details of lumazine synthase and riboflavin synthase catalysis. The following is a list of the main results: (1) All of the synthesized metabolically stable oxalamic acid derivative probes with S, O, and NH linkages between the ribityl side chain and pyrimidinedione ring that are analogues of the phosphate elimination products of the lumazine synthase reaction intermediate **6** are moderate or inactive lumazine synthase inhibitors. However, compounds containing a phosphate side chain have very strong affinity for lumazine synthase. This suggests that lumazine synthase predominantly catalyzes Schiff base formation and the phosphate elimination reaction, and the subsequent intermediates have low enzyme affinity (Scheme 2). (2) Compounds **76**, **77**, and **78**, which do not contain either the phosphate side chain or the ribityl side chain, showed very weak or complete absence of any inhibitory activity. Whereas compound **75**[41] lacks the ribityl side chain, it has a phosphate group that binds to the phosphate binding site, resulting in strong affinity for lumazine synthase (K_d of 0.72 μM vs *M. tuberculosis* lumazine synthase). This suggests that the pyrimidinedione ring alone has low binding affinity, and the phosphate moiety contributes more positively to the binding of compound compared to the ribityl side chain. Previously reported work has shown that the ribityl side chain can be replaced by a styryl moiety with retention of affinity for the enzyme, indicating that the ribityl chain is not essential for binding.[59] (3) Among all of the compounds synthesized, *S*-nucleoside **23** showed greater lumazine synthase inhibitory potency (Table 1) as compared to all the *O*-nucleoside, *N*-nucleoside, and *C*-nucleoside derivatives. The greater inhibitory potency of the *S*-nucleoside **23** and its nitro precursor **24** compared with the *O*-nucleoside **29** and *C*-nucleoside **74** could possibly be due to electronics. The nonbonded electrons on sulfur would cause **23** to more closely resemble the natural substrate relative to the *C*-nucleoside **74**. (4) All of the bicyclic compounds (**69**, **81**, and **84**) were found to exhibit stronger affinity for riboflavin synthase than lumazine synthase. (5) The molecular dynamics simulations provide a method for predicting ligand affinities to the active site of lumazine synthase. They also provide insight into the dynamic aspects of ligand binding. (6) A useful controlled hydrogenolysis methodology has been developed and applied to the selective cleavage of benzyl protecting groups in the presence of easily reducible functional groups. The information revealed in this study will be valuable for future structure-based drug design of lumazine synthase and riboflavin synthase inhibitors.

EXPERIMENTAL SECTION

General. Melting points were determined using capillary tubes and are uncorrected. NMR spectra were determined at 300 or 500 MHz (^{1}H) and 75 or 125 MHz (^{13}C) as specified. High-resolution mass spectra were recorded on a double-focusing sector mass spectrometer with magnetic and electrostatic mass analyzers. Silica gel flash chromatography was performed using 230–400 mesh silica gel.

2,4-Bis(benzyloxy)-5-nitro-6-(((4*R*,4′*R*,5*S*)-2,2,2′,2′-tetramethyl-4,4′-bi(1,3-dioxolan)-5-yl)methoxy)pyrimidine (27). A solution of D-ribitol derivative **26** (62 mg, 0.27 mmol) in dry THF (5 mL) was cooled to −40 °C, and LiHMDS (0.3 mL, 1 M solution in THF, 0.32 mmol) was added. The solution was stirred for 30 min at room temperature and cooled to −40 °C. Chloropyrimidine derivative **25** (100 mg, 0.27 mmol) dissolved in dry THF (5 mL) was introduced into the reaction mixture, which was slowly brought to room

temperature over 5 h. The reaction was quenched using ammonium chloride, THF was removed under vacuum, the residue then dissolved in CHCl$_3$ (15 mL), and the organic layer was washed with water and brine, dried, and concentrated. The residue was purified by silica gel flash column chromatography, eluting with 15% ethyl acetate in hexane, to yield compound **27** (108 mg, 71%) as a colorless oil: ^{1}H NMR (300 MHz, CDCl$_3$) δ 7.33–7.24 (m, 10 H), 5.48 (s, 2 H), 5.40 (s, 2 H), 4.79 (dd, *J* = 3.9 Hz, 11.5 Hz, 1 H), 4.61 (dd, *J* = 6.2 Hz, 11.5 Hz, 1 H), 4.52–4.47 (m, 1 H), 4.16–4.01 (m, 3 H), 3.93–3.85 (m, 1 H), 1.39 (s, 3 H), 1.34 (s, 3 H), 1.32 (s, 3 H), 1.23 (s, 3 H); ^{13}C NMR (75 MHz, CDCl$_3$) δ 163.8, 162.0, 135.4, 135.0, 128.6, 128.3, 128.2, 127.6, 109.8, 109.4, 77.7, 75.0, 73.3, 70.3, 69.8, 68.0, 66.8, 27.6, 26.7, 25.3, 25.2. Anal. Calcd for C$_{29}$H$_{33}$N$_3$O$_9$: C, 61.37; H, 5.86; N, 7.40. Found: C, 61.44; H, 5.88; N, 7.36.

(2*R*,3*R*,4*S*)-5-(2,6-Bis(benzyloxy)-5-nitropyrimidin-4-yloxy)-pentane-1,2,3,4-tetrol (28). HCl (0.5 N, 2 mL) was added to a solution of compound **27** (50 mg, 0.09 mmol) in THF (2 mL), and the reaction mixture was stirred for 6 h at room temperature. THF was removed under vacuum, the residue then dissolved in ethyl acetate (10 mL), and the organic layer was washed with water and brine, dried, and concentrated. The residue was purified by silica gel flash column chromatography, eluting with 60% ethyl acetate in hexane, to afford compound **28** (31 mg, 72%) as a colorless oil: ^{1}H NMR (300 MHz, CDCl$_3$) δ 7.35–7.27 (m, 10 H), 5.46 (s, 2 H), 5.38 (s, 2 H), 4.68 (dd, *J* = 2.9 Hz, 11.3 Hz, 1 H) 4.55 (dd, *J* = 6.2 Hz, 11.3 Hz, 1 H), 4.06–4.00 (m, 1 H), 3.76–3.63 (m, 4 H); ^{13}C NMR (75 MHz, CDCl$_3$) δ 164.0, 163.5, 161.8, 135.0, 134.7, 128.2, 128.0, 127.7, 127.2, 72.4, 71.3, 70.6, 70.1, 70.0, 69.6, 62.9; ESIMS *m/z* (rel. intensity) 997 (2MNa$^+$, 100), 863 (30), 510 (MNa$^+$, 42). Anal. Calcd for C$_{23}$H$_{25}$N$_3$O$_9$: C, 56.67; H, 5.17; N, 8.62. Found: C, 56.81; H, 5.21; N, 8.49.

5-Amino-6-((2*R*,3*R*,4*S*)-2,3,4,5-tetrahydroxypentyloxy)-pyrimidine-2,4(1*H*,3*H*)-dione (29). Pd/C (10%, 5 mg) was added to a solution of compound **28** (45 mg, 0.08 mmol) in MeOH/EtOAc (3 + 1 mL). A hydrogen balloon was attached, and the mixture was stirred at room temperature for 12 h. The reaction mixture was filtered through Celite into a solution of MeOH containing HCl. The solution was concentrated to provide compound **29** (24 mg, 83%) as yellow amorphous solid: mp 200−204 °C (dec); ^{1}H NMR (300 MHz, MeOH-d_4) δ 4.14−4.08 (m, 1 H), 3.97 (dd, *J* = 4.8 Hz, 9.5 Hz, 1 H), 3.71−3.68 (m, 4 H), 3.52 (dd, *J* = 4.8 Hz, 12.0 Hz, 1 H); ^{13}C NMR (75 MHz, MeOH-d_4) δ 168.3, 166.0, 158.9, 108.8, 84.1, 73.8, 73.1, 72.5, 63.2; ESIMS *m/z* (rel. intensity) 278 (MH$^+$, 35); negative ion ESIMS *m/z* (rel. intensity) 276 [(M − H$^+$)$^-$, 62], 171 (100). Anal. Calcd for C$_9$H$_{16}$ClN$_3$O$_7$: C, 34.46; H, 5.14; N, 13.40. Found: C, 34.12; H, 5.18; N, 13.52.

5-Nitro-6-((2*S*,3*R*,4*R*)-2,3,4,5-tetrahydroxypentyloxy)-pyrimidine-2,4(1*H*,3*H*)-dione (22). Lindlar catalyst (5 mg) was added to a solution of compound **28** (45 mg, 0.08 mmol) in MeOH/EtOAc (3 + 1 mL). A hydrogen balloon was attached, and the mixture was stirred at room temperature for 12 h. The reaction mixture was filtered through Celite, which was then washed with 50% aq MeOH (5 mL). The solution was concentrated, and the residue was purified via silica gel flash column chromatography, eluting with 10% methanol in ethyl acetate, to furnish compound **22** as a colorless oil. Compound **22** was washed several times with CH$_2$Cl$_2$ and THF. Finally, compound **22** was precipitated out by dissolving in MeOH and adding excess diethyl ether to afford pure compound **22** (22 mg, 79%) as an orange amorphous solid: mp 165−168 °C (dec); ^{1}H NMR (300 MHz, MeOH-d_4) δ 4.15−4.106 (m, 1 H), 4.03−3.94 (m, 3 H), 3.78−3.68 (m, 2 H), 3.68 (dd, *J* = 9.5 Hz, 14.0 Hz, 1 H); ^{13}C NMR (75 MHz, MeOH-d_4) δ 167.9, 164.2, 157.6, 123.0, 79.8, 79.6, 74.5, 68.4, 62.2; negative ion ESIMS *m/z* (rel. intensity) 306 [(M − H$^+$)$^-$, 100], 172 (65). Anal. Calcd for C$_9$H$_{13}$N$_3$O$_9$: C, 35.19; H, 4.27; N, 13.68. Found: C, 34.97; H, 4.43; N, 13.90.

2,4-Dimethoxy-5-nitro-6-(((4*R*,4′*R*,5*S*)-2,2,2′,2′-tetramethyl-4,4′-bi(1,3-dioxolan)-5-yl)methoxy)pyrimidine (31). A solution of D-ribitol derivative **26** (100 mg, 0.43 mmol) in dry THF (8 mL) was cooled to −40 °C and *n*-BuLi (0.3 mL, 2.5 M, 0.86 mmol) was added. The solution was stirred for 30 min at room temperature and cooled to −40 °C. Iodopyrimidine derivative **30** (122 mg, 0.39 mmol) dissolved in

dry THF (8 mL) was introduced into the reaction mixture, which was slowly brought to room temperature by overnight stirring. The reaction was quenched using ammonium chloride, THF was removed under vacuum, the residue then dissolved in CHCl$_3$ (15 mL), and the organic layer was washed with water and brine, dried, and concentrated. The residue was column chromatographed with flash silica gel eluting with 20% ethyl acetate in hexane to yield compound **31** (75 mg, 45%) as a colorless oil along with both the staring materials **30** and **26**: ^{1}H NMR (300 MHz, CDCl$_3$) δ 4.81 (dd, J = 4.1 Hz, 1 H), 4.64 (dd, J = 6.0 Hz, 1 H), 4.50−4.47 (m, 1 H), 4.16−4.06 (m, 3 H), 4.05 (s, 3 H), 4.00 (s, 3 H), 3.92−3.86 (m, 1 H), 1.37 (s, 3 H), 1.33 (s, 3 H), 1.31 (s, 3 H), 1.23 (s, 3 H); ^{13}C NMR (75 MHz, CDCl$_3$) δ 164.4, 163.8, 162.7, 109.7, 109.4, 77.7, 75.1, 73.3, 68.0, 66.7, 55.6, 55.5, 27.5, 26.7, 25.2; EIMS m/z (rel. intensity) 400 (M$^+$ − CH$_3$, 11), 256 (C$_9$H$_{10}$N$_3$O$_6$$^+$, 20), 101 (C$_5H_5O_2$$^+$, 100); CIMS m/z (rel. intensity) 416 (MH$^+$, 14), 215 (M$^+$ − C$_{11}$H$_{19}$O$_4$, 100). Anal. Calcd for C$_{17}$H$_{25}$N$_3$O$_9$: C, 49.15; H, 6.07; N, 10.12. Found: C, 49.44; H, 5.88; N, 10.34.

2,4-Bis(benzyloxy)-6-(((4R,4′R,5S)-2,2,2′,2′-tetramethyl-4,4′-bi(1,3-dioxolan)-5-yl)methoxy)pyrimidin-5-amine (32). Sodium bicarbonate−sodium carbonate buffer (3 mL) (pH = 9.5, prepared by adjusting the pH value of saturated sodium carbonate aqueous solution to 9.5 with sodium carbonate and 1 M NaOH) and Na$_2$S$_2$O$_4$ (260 mg, 1.48 mmol) were added to a solution of compound **27** (120 mg, 0.211 mmol) in 1,4-dioxane (3 mL). Argon was bubbled for 20 min to degas the reaction mixture, which was stirred at room temperature for 6 h and subsequently at 100 °C for 3 h. The reaction mixture was cooled to room temperature and poured into ice water (5 mL) and extracted with diethyl ether (3 × 8 mL). The organic layer was combined, washed with brine, dried, and solvent was distilled off. The residue was separated by flash chromatography eluting with 20% ethyl acetate in hexane, to yield compound **32** (82 mg, 72%) as light yellow oil: ^{1}H NMR (300 MHz, CDCl$_3$) δ 7.42−7.18 (m, 10 H), 5.33 (s, 2 H), 5.25 (s, 2 H), 4.59 (dd, J = 10.41 Hz, 3.58 Hz, 1 H), 4.48−4.38 (m, 2 H), 4.13−3.95 (m, 4 H), 3.91−3.82 (m, 1 H), 3.21 (brs, 2 H), 1.46 (s, 3 H), 1.37 (s, 3 H), 1.28 (s, 3 H), 1.22 (s, 3 H); ^{13}C NMR (75 MHz, CDCl$_3$) δ 158.5, 158.3, 155.0, 137.2, 136.7, 128.4, 128.3, 128.1, 128.0, 127.8, 109.7, 109.1, 107.7, 77.9, 75.6, 73.2, 68.7, 68.4, 68.0, 65.2, 27.9, 26.8, 25.5, 25.3; ESIMS m/z (rel. intensity) 560 (MNa$^+$, 100), 538 (MH$^+$, 50), 480 (9). Anal. Calcd for C$_{29}$H$_{35}$N$_3$O$_7$: C, 64.79; H, 6.56; N, 7.82. Found: C, 65.03; H, 6.41; N, 7.64.

Ethyl 2-(2,4-Bis(benzyloxy)-6-(((4R,4′R,5S)-2,2,2′,2′-tetramethyl-4,4′-bi(1,3-dioxolan)-5-yl)methoxy)pyrimidin-5-ylamino)-2-oxoacetate (33). Triethylamine (0.3 mL, 2.2 mmol) was added to a solution of compound **32** (30 mg, 0.055 mmol) in THF (5 mL). The solution was cooled to 0 °C, and ethyl chlorooxacetate (18 μL, 0.16 mmol) was added dropwise. The reaction mixture was stirred at 0 °C for 2 h and 30 min at room temperature. The solvent was distilled off under reduced pressure, and the residue was dissolved in dichloromethane (20 mL) and washed with water (2 × 15 mL). The organic layer was dried and solvent was distilled off. The residue was separated by silica gel flash column chromatography, eluting with 30% ethyl acetate in hexane, to afford compound **33** (36 mg, 96%) as a yellowish oil: ^{1}H NMR (300 MHz, CDCl$_3$) δ 8.11 (s, 1 H), 7.41−7.19 (m, 10 H), 5.37 (s, 2 H), 5.32 (s, 2 H), 4.67−4.59 (m, 1 H), 4.47−4.42 (m, 2 H), 4.32 (q, J = 7.16 Hz, 2 H), 4.06−3.96 (m, 3 H), 3.89−3.83 (m, 1 H), 1.34 (s, 3 H), 1.33 (t, J = 7.1 Hz, 3 H), 1.30 (s, 3 H), 1.25 (s, 3 H), 1.19 (s, 3 H); ^{13}C NMR (75 MHz, CDCl$_3$) δ 165.9, 161.6, 160.2, 154.7, 136.2, 136.1, 128.4, 128.2, 128.0, 127.7, 109.8, 109.2, 95.6, 77.7, 75.3, 73.2, 69.5, 69.0, 67.9, 66.0, 63.3, 27.7, 26.8, 25.3, 25.2, 14.0; ESIMS m/z (rel. intensity) 660 (MNa$^+$, 100), 446 (2). Anal. Calcd for C$_{33}$H$_{39}$N$_3$O$_{10}$: C, 62.16; H, 6.16; N, 6.59. Found: C, 62.34; H, 6.30; N, 6.88.

Ethyl 2-(2,4-Bis(benzyloxy)-6-((2S,3R,4R)-2,3,4,5-tetrahydroxypentyloxy)pyrimidin-5-ylamino)-2-oxoacetate (34) and Methyl 2-(2,4-Bis(benzyloxy)-6-((2S,3R,4R)-2,3,4,5-tetrahydroxypentyloxy)pyrimidin-5-ylamino)-2-oxoacetate (35). HCl (0.5 N, 1 mL) was added to a solution of compound **33** (35 mg, 0.055 mmol) in MeOH (1 mL), and the reaction mixture was stirred for 12 h at room temperature. MeOH was removed under vacuum, the residue then dissolved in ethyl acetate (10 mL), and the organic layer was washed with water and brine, dried, and concentrated. The residue

was purified by silica gel flash column chromatography, eluting with 70% ethyl acetate in hexane, to give compounds **34** (16 mg, 53%) and **35** (11 mg, 37%) as a colorless oils. Compound **34**: ^{1}H NMR (300 MHz, acetone-d_6) δ 9.36 (s, 1 H), 7.50−7.30 (m, 10 H), 5.46 (s, 2 H), 5.40 (s, 2 H), 4.74−4.69 (m, 1 H), 4.53−4.48 (m, 1 H), 4.42 (brs, 1 H), 4.31 (q, J = 7.12 Hz, 2 H), 4.14−4.03 (m, 3 H), 3.77−3.67 (m, 4 H), 1.34 (t, J = 7.12 Hz); ^{13}C NMR (75 MHz, CDCl$_3$) δ 165.6, 165.2, 159.9, 154.8, 136.0, 135.5, 128.6, 128.3, 128.2, 128.1, 95.6, 73.2, 71.5, 69.8, 69.3, 63.8, 63.3, 13.9; ESIMS m/z (rel. intensity) 1137 (2 M + Na$^+$, 100), 580 (MNa$^+$, 69), 559 (M2H$^+$, 12), 558 (MH$^+$, 47). Anal. Calcd for C$_{27}$H$_{31}$N$_3$O$_{10}$: C, 58.16; H, 5.60; N, 7.54. Found: C, 57.82; H, 5.88; N, 7.21.

Compound **35**: ^{1}H NMR (300 MHz, acetone-d_6) δ 9.42 (s, 1 H), 7.47−7.32 (m, 10 H), 5.46 (s, 2 H), 5.40 (s, 2 H), 4.75−4.68 (m, 1 H), 4.52−4.45 (m, 2 H), 4.19 (brs, 1 H), 4.10−4.08 (m, 2 H), 3.85 (s, 3 H), 3.75−3.70 (m, 3 H), 3.68−3.64 (m, 2 H), 3.58 (m, 1 H), 3.42 (m, 1 H); ^{13}C NMR (75 MHz, acetone-d_6) δ 167.4, 167.1, 161.5, 156.2, 137.7, 137.6, 129.2, 129.0, 128.8, 128.7, 128.5, 96.9, 73.7, 73.4, 71.8, 70.2, 70.0, 69.3, 64.5, 53.6; ESIMS m/z (rel. intensity) 566 (MNa$^+$, 100), 504 (8), 303 (8); negative ion ESIMS m/z (rel. intensity) 542 [(M − H$^+$)$^−$, 100], 408 (59). Anal. Calcd for C$_{26}$H$_{29}$N$_3$O$_{10}$: C, 57.45; H, 5.38; N, 7.73. Found: C, 57.69; H, 5.18; N, 7.66.

Ethyl 2-(2,4-Dioxo-6-((2S,3R,4R)-2,3,4,5-tetrahydroxypentyloxy)-1,2,3,4-tetrahydropyrimidin-5-ylamino)-2-oxoacetate (36). Pd/C (10%, 5 mg) was added to a solution of compound **34** (30 mg, 0.054 mmol) in EtOH (4 mL). A hydrogen balloon was attached, and the mixture was stirred at room temperature for 12 h. The reaction mixture was filtered through Celite, which was then washed with EtOH (15 mL) and the filtrate concentrated to provide compound **36** (14 mg, 70%) as white solid: mp 62−64 °C; ^{1}H NMR (300 MHz, MeOH-d_4) δ 4.52−4.47 (m, 1 H), 4.46−4.40 (m, 1 H), 4.34 (q, J = 7.10 Hz, 2 H), 4.02−3.98 (m, 1 H), 3.77−3.70 (m, 2 H), 3.67−3.61 (m, 2 H), 1.34 (t, J = 7.10 Hz, 3 H); ^{13}C NMR (75 MHz, MeOH-d_4) δ 164.7, 162.4, 161.1, 159.2, 153.1, 93.2, 74.1, 74.0, 73.1, 72.5, 64.5, 64.1, 14.3; ESIMS m/z (rel. intensity) 777 (2 M + Na$^+$, 100), 400 (MNa$^+$, 32), 378 (MH$^+$, 16); negative ion ESIMS m/z (rel. intensity) 752 [(2 M − H$^+$)$^−$, 42], 376 [(M − H$^+$)$^−$, 100], 241 (60). Anal. Calcd for C$_{13}$H$_{19}$N$_3$O$_{10}$·H$_2$O: C, 39.50; H, 5.35; N, 10.63. Found: C, 39.67; H, 5.17; N, 10.40.

Methyl 2-(2,4-Dioxo-6-((2S,3R,4R)-2,3,4,5-tetrahydroxypentyloxy)-1,2,3,4-tetrahydropyrimidin-5-ylamino)-2-oxoacetate (37). Pd/C (10%, 3 mg) was added to a solution of compound **35** (20 mg, 0.037 mmol) in MeOH (3 mL). A hydrogen balloon was attached, and the mixture was stirred at room temperature for 12 h. The reaction mixture was filtered through Celite, which was then washed with MeOH (15 mL) and concentrated to provide compound **37** (10 mg, 75%) as a colorless oil: ^{1}H NMR (300 MHz, MeOH-d_4) δ 4.49−4.42 (m, 2 H), 3.95−3.90 (m, 1 H), 3.88 (s, 3 H), 3.76−3.71 (m, 2 H), 3.64−3.58 (m, 2 H); ^{13}C NMR (75 MHz, MeOH-d_4) δ 168.2, 165.3, 160.7, 152.0, 91.3, 74.2, 74.1, 73.4, 72.8, 69.1, 64.5; ESIMS m/z (rel. intensity) 386 (MNa$^+$, 94), 256 (93), 179 (100); negative ion ESIMS m/z (rel. intensity) 362 [(M − H$^+$)$^−$, 100], 348 (8), 231 (7). Anal. Calcd for C$_{12}$H$_{17}$N$_3$O$_{10}$·2H$_2$O: C, 36.10; H, 5.30; N, 10.52. Found: C, 36.33; H, 5.43; N, 10.49.

N-(2,4-Bis(benzyloxy)-6-(((4R,4′R,5S)-2,2,2′,2′-tetramethyl-4,4′-bi(1,3-dioxolan)-5-yl)methoxy)pyrimidin-5-yl)-isobutyramide (38). Triethylamine (0.3 mL, 2.2 mmol) was added to a solution of compound **32** (115 mg, 0.21 mmol) in THF (5 mL). The solution was cooled to 0 °C, and isobutyryl chloride (25 μL, 0.24 mmol) was added dropwise. The reaction mixture was stirred at 0 °C for 6 h. The solvent was distilled off under reduced pressure, and the residue was dissolved in dichloromethane (20 mL) and washed with water (2 × 15 mL). The organic layer was dried and solvent was distilled off. The residue was flash column chromatographed with flash silica gel, eluting with 35% ethyl acetate in hexane, to afford compound **38** (110 mg, 85%) as a yellowish-white solid: mp 150−153 °C; ^{1}H NMR (300 MHz, CDCl$_3$) δ 7.43−7.24 (m, 10 H), 6.53 (s, 1 H), 5.34 (s, 4 H), 4.68 (dd, J = 2.1, 10.5 Hz, 1 H), 4.47−4.39 (m, 2 H), 4.08−4.0 (m, 3 H), 3.92−3.89 (m, 1 H), 2.47 (m, 1 H), 1.39 (s, 3 H), 1.35 (s, 3 H), 1.30 (s, 3 H), 1.26 (s, 3 H), 1.17 (m, 6 H); ^{13}C NMR (75 MHz, CDCl$_3$) δ 175.6, 166.4, 166.1, 161.0, 136.3, 136.2, 128.2, 128.1, 127.9, 127.7, 127.4, 109.6, 109.0,

97.0, 77.5, 75.4, 73.1, 69.2, 68.6, 67.7, 65.7, 35.3, 27.6, 26.7, 25.2, 19.5, 19.3; ESIMS m/z (rel. intensity) 608 (MH$^+$, 100), 550 (14); HRMS m/z calcd for $C_{33}H_{42}N_3O_8$ (MH$^+$) 608.2972, found 608.2981. Anal. Calcd for $C_{33}H_{41}N_3O_8$: C, 65.22; H, 6.80; N, 6.91. Found: C, 65.40; H, 6.53; N, 7.12.

N-(2,4-Bis(benzyloxy)-6-((2S,3R,4R)-2,3,4,5-tetrahydroxypentyloxy)pyrimidin-5-ylamino)isobutyramide (39). HCl (0.5 N, 1 mL) was added to a solution of compound **38** (60 mg, 0.1 mmol) in THF (2 mL), and the reaction mixture was stirred for 12 h at room temperature. THF was removed under vacuum, the residue then dissolved in ethyl acetate (10 mL), and the organic layer was washed with water and brine, dried, and concentrated. The residue was column chromatographed with flash silica gel, eluting with 80% ethyl acetate in hexane, to produce compound **39** (43 mg, 81%) as white semisolid: ^{1}H NMR (300 MHz, MeOH-d_4) δ 7.42−7.29 (m, 10 H), 5.38 (s, 4 H), 4.61 (m, 1 H), 4.58 (dd, J = 4.5, 8.1 Hz, 1 H), 4.46 (dd, J = 6.6, 11.4 Hz, 1 H), 3.78−3.65 (m, 2 H), 3.68−3.62 (m, 2 H), 2.68−2.50 (m, 1 H), 1.17 (d, J = 1.2 Hz, 3 H), 1.15 (d, J = 1.2 Hz, 1 H); ^{13}C NMR (75 MHz, MeOH-d_4) δ 180.1, 168.4, 168.0, 162.9, 138.2, 137.9, 129.7, 129.5, 129.4, 129.1, 128.8, 128.6, 98.2, 84.1, 74.2, 73.5, 72.1, 70.5, 70.0, 64.6, 36.2, 19.9; ESIMS m/z (rel. intensity) 550 (MNa$^+$, 100), 528 (MH$^+$, 68), 394 (36); negative ion ESIMS m/z (rel. intensity) 526 [(M − H$^+$)$^-$, 28], 392 (100). Anal. Calcd for $C_{27}H_{33}N_3O_8$: C, 61.47; H, 6.30; N, 7.96. Found: C, 61.65; H, 6.31; N, 7.80.

N-(2,4-Dioxo)-6-((2S,3R,4R)-2,3,4,5-tetrahydroxypentyloxy)-1,2,3,4-tetrahydropyrimidin-5-yl)isobutyramide (40). Pd/C (10%, 5 mg) was added to a solution of compound **39** (55 mg, 0.08 mmol) in MeOH/EtOAc (3 + 1 mL). A hydrogen balloon was attached, and the mixture was stirred at room temperature for 12 h. The reaction mixture was filtered through Celite into a solution of MeOH containing HCl. The solution was concentrated to provide compound **40** (26 mg, 72%) as yellow amorphous solid: mp 116−119 °C; ^{1}H NMR (300 MHz, MeOH-d_4) δ 4.47−4.41 (m, 2 H), 3.97−3.90 (m, 1 H), 3.77−3.71 (m, 2 H), 3.64−3.60 (m, 2 H), 2.66−2.59 (m, 1 H), 1.19 (s, 3 H), 1.17 (s, 3 H); ^{13}C NMR (75 MHz, MeOH-d_4) δ 180.9, 165.8, 165.26, 156.0, 93.5, 74.2, 73.2, 72.7, 72.0, 64.5, 36.2, 20.0; ESIMS m/z (rel. intensity) 370 (MNa$^+$, 100), 300 (11), 219 (16); negative ion ESIMS m/z (rel. intensity) 346 [(M − H$^+$)$^-$, 100], 212 (6). Anal. Calcd for $C_{13}H_{21}N_3O_8$: C, 44.96; H, 6.09; N, 12.10. Found: C, 45.11; H, 5.93; N, 11.86.

N-(2,4-Bis(benzyloxy)-6-(((4R,4'R,5S)-2,2,2',2'-tetramethyl-4,4'-bi(1,3-dioxolan)-5-yl)methoxy)pyrimidin-5-yl)-propionamide (41). Triethylamine (0.3 mL, 2.2 mmol) was added to a solution of compound **32** (80 mg, 0.15 mmol) in THF (5 mL). The solution was cooled to 0 °C and propionyl chloride (16 μL, 0.18 mmol) was added dropwise. The reaction mixture was stirred at 0 °C for 6 h. The solvent was distilled off under reduced pressure, and the residue was dissolved in dichloromethane (20 mL) and washed with water (2 × 15 mL). The organic layer was dried, and solvent was distilled off. The residue was flash column chromatographed with flash silica gel, eluting with 35% ethyl acetate in hexane, to afford compound **41** (77 mg, 87%) as a yellowish-white solid: mp 121−123 °C; ^{1}H NMR (300 MHz, CDCl$_3$) δ 7.38−7.25 (m, 10 H), 6.42 (s, 1 H), 5.31−5.28 (m, 4 H), 4.62 (dd, J = 2.4, 10.5 Hz, 1 H), 4.45−4.41 (m, 2 H), 4.04−3.98 (m, 3 H), 3.86−3.85 (m,1 H), 2.25 (q, J = 7.4 Hz, 2 H), 1.34 (s, 3 H), 1.30 (s, 3 H), 1.25 (s, 3 H), 1.21 (s, 3 H), 1.14 (t, J = 7.2 Hz, 3 H); ^{13}C NMR (125 MHz, CDCl$_3$) δ 172.6, 166.5, 166.2, 161.1, 136.3, 136.2, 128.7, 128.5, 128.4, 128.1, 127.9, 127.6, 127.5, 109.8, 109.2, 97.1, 77.7, 75.7, 73.4, 69.3, 68.7, 67.8, 65.9, 29.7, 27.7, 26.9, 25.2; ESIMS m/z (rel. intensity) 594 (MH$^+$, 100), 554 (27), 245 (35); HRMS m/z calcd for $C_{32}H_{40}N_3O_8$ (MH$^+$) 594.2815, found 594.2825. Anal. Calcd for $C_{32}H_{39}N_3O_8$: C, 64.74; H, 6.62; N, 7.08. Found: C, 64.88; H, 6.85; N, 6.81.

N-(2,4-Bis(benzyloxy)-6-((2S,3R,4R)-2,3,4,5-tetrahydroxypentyloxy)pyrimidin-5-ylamino)propionamide (42). HCl (0.5 N, 1 mL) was added to a solution of compound **41** (60 mg, 0.1 mmol) in MeOH (1 mL), and the reaction mixture was stirred for 12 h at room temperature. MeOH was removed under vacuum, the residue then dissolved in ethyl acetate (10 mL), and the organic layer was washed with water and brine, dried, and concentrated. The residue was flash column chromatographed with silica gel, eluting with 80% ethyl acetate in hexane, to afford compound **42** (39 mg, 75%) as white

solid: mp 110−113 °C; ^{1}H NMR (300 MHz, MeOH-d_4) δ 7.43−7.31 (m, 10 H), 5.38 (s, 4 H), 4.62−4.58 (m, 1 H), 4.46 (dd, J = 2.7, 10.8 Hz, 1 H), 4.08−4.02 (m, 1 H), 3.79−3.76 (m, 2 H), 3.69−3.61 (m, 2 H), 2.36 (q, J = 7.4 Hz, 2 H), 1.17 (t, J = 7.2 Hz, 3 H); ^{13}C NMR (75 MHz, MeOH-d_4) δ 177.4, 168.8, 168.4, 163.3, 138.6, 138.4, 130.0, 129.5, 129.2, 98.7, 74.6, 74.0, 72.5, 71.0, 70.4, 65.0, 30.5, 11.0; ESIMS m/z (rel. intensity) 536 (MNa$^+$, 100), 514 (MH$^+$, 10); negative ion ESIMS m/z (rel. intensity) 512 [M − H$^+$)$^-$, 4], 462 (100); HRMS m/z calcd for $C_{26}H_{31}N_3O_8Na$ (MNa$^+$) 536.2009, found 536.2011. Anal. Calcd for $C_{26}H_{31}N_3O_8$: C, 60.81; H, 6.08; N, 8.18. Found: C, 60.95; H, 6.31; N, 8.02.

N-(2,4-Dioxo-6-((2S,3R,4R)-2,3,4,5-tetrahydroxypentyloxy)-1,2,3,4-tetrahydropyrimidin-5-yl)propionamide (43). Pd/C (10%, 5 mg) was added to a solution of compound **42** (55 mg, 0.08 mmol) in MeOH/EtOAc (3 + 1 mL). A hydrogen balloon was attached, and the mixture was stirred at room temperature for 12 h. The reaction mixture was filtered through Celite into a solution of MeOH containing HCl. The solution was concentrated to provide compound **43** (25 mg, 70%) as yellow amorphous solid: mp 128−131 °C; ^{1}H NMR (300 MHz, MeOH-d_4) δ 4.62−4.58 (m, 1 H), 4.49−4.43 (m, 1 H), 4.06−4.02 (m, 1 H), 3.80−3.75 (m, 2 H), 3.67−3.61 (m, 2 H), 2.38 (q, J = 7.4 Hz, 2 H), 1.16 (t, J = 7.3 Hz, 3 H); ^{13}C NMR (75 MHz, MeOH-d_4) δ 178.5, 163.7, 162.8, 156.0, 85.0, 72.4, 71.2, 70.7, 64.5, 30.1, 29.4, 10.5. Anal. Calcd for $C_{12}H_{19}N_3O_8$: C, 43.24; H, 5.75; N, 12.61. Found: C, 43.10; H, 5.72; N, 12.89.

N-(2,4-Bis(benzyloxy)-6-(((4R,4'R,5S)-2,2,2',2'-tetramethyl-4,4'-bi(1,3-dioxolan)-5-yl)methoxy)pyrimidin-5-yl)-methacrylamide (44). Triethylamine (0.3 mL, 2.2 mmol) was added to a solution of compound **32** (115 mg, 0.21 mmol) in THF (5 mL). The solution was cooled to 0 °C and methacroyl chloride (25 μL, 0.24 mmol) was added dropwise. The reaction mixture was stirred at 0 °C for 6 h. The solvent was distilled off under reduced pressure, and the residue was dissolved in dichloromethane (20 mL) and washed with water (2 × 15 mL). The organic layer was dried, and solvent was distilled off. The residue was flash column chromatographed with silica gel, eluting with 35% ethyl acetate in hexane, to afford compound **44** (85 mg, 65%) as white amorphous solid: mp 118−120 °C; ^{1}H NMR (300 MHz, CDCl$_3$) δ 7.42−7.24 (m, 10 H), 6.81 (s, 1 H), 5.72 (s, 1 H), 5.37 (s, 2 H), 5.34 (s, 1 H), 5.33 (s, 2 H), 4.67 (dd, J = 1.8, 8.1 Hz, 1 H), 4.49−4.42 (m, 2 H), 4.15−4.00 (m, 3 H), 3.89 (dd, J = 4.8, 8.1 Hz 1 H), 1.97 (s, 3 H), 1.38 (s, 3 H), 1.34 (s, 3 H), 1.29 (s, 3 H), 1.24 (s, 3 H); ^{13}C NMR (75 MHz, CDCl$_3$) δ 167.2, 166.3, 166.2, 161.1, 140.1, 136.3, 128.3, 128.1, 128.0, 127.8, 127.4, 119.8, 109.6, 109.0, 97.0, 77.6, 75.4, 73.2, 69.3, 68.6, 67.8, 65.8, 27.5, 26.7, 25.2, 18.7; ESIMS m/z (rel. intensity) 606 (MH$^+$, 100), 550 (59), 538 (21); HRMS m/z calcd for $C_{33}H_{40}N_3O_8$ (MH$^+$) 606.2851, found 606.2812. Anal. Calcd for $C_{33}H_{39}N_3O_8$: C, 65.44; H, 6.49; N, 6.94. Found: C, 65.51; H, 6.62; N, 7.09.

N-(2,4-Bis(benzyloxy)-6-((2S,3R,4R)-2,3,4,5-tetrahydroxypentyloxy)pyrimidin-5-ylamino)methacrylamide (45). HCl (0.5 N, 1 mL) was added to a solution of compound **44** (60 mg, 0.1 mmol) in MeOH (1 mL), and the reaction mixture was stirred for 12 h at room temperature. MeOH was removed under vacuum, the residue was then dissolved in ethyl acetate (10 mL), and the organic layer was washed with water and brine, dried, and concentrated. The residue was flash column chromatographed with silica gel, eluting with 80% ethyl acetate in hexane, to provide compound **45** (36 mg, 69%) as a colorless oil: ^{1}H NMR (300 MHz, MeOH-d_4) δ 7.40−7.27 (m, 10 H), 5.84 (s, 1 H), 5.48 (s, 1 H), 5.40 (s, 2 H), 5.38 (s, 2 H), 4.62 (dd, J = 3.0, 11.4 Hz, 1 H), 4.47 (dd, J = 6.6, 11.4 Hz, 1 H) 4.06−4.05 (m, 1 H), 3.79−3.77 (m, 2 H), 3.75−3.73 (m, 2 H), 1.99 (s, 3 H); ^{13}C NMR (75 MHz, MeOH-d_4) δ 170.9, 168.5, 168.1, 163.0, 141.1, 138.1, 138.0, 129.5, 129.4, 129.1, 129.0, 128.6, 128.4, 121.7, 98.3, 74.1, 73.5, 72.0, 70.5, 70.0, 69.9, 64.6, 18.9; ESIMS m/z (rel. intensity) 526 (MH$^+$, 100), 494 (24), 392 (42); negative ion ESIMS m/z (rel. intensity) 524 [(M − H$^+$)$^-$, 24], 391 (21), 390 (100). Anal. Calcd for $C_{27}H_{31}N_3O_8$: C, 61.70; H, 5.95; N, 8.00. Found: C, 61.91; H, 5.90; N, 7.88.

N-(2,4-Dioxo-6-((2S,3R,4R)-2,3,4,5-tetrahydroxypentyloxy)-1,2,3,4-tetrahydropyrimidin-5-yl)methacrylamide (46). Lindlar catalyst (5 mg) was added to a solution of compound **45** (50 mg, 0.095 mmol) in anhydrous ethanol (4 mL). 1,4-Cyclohexadiene (52 μL, 0.95

mmol) was added, and argon was bubbled through the reaction mixture for 10 min. The mixture was stirred at room temperature for 12 h. The reaction mixture was filtered through Celite, which was then washed with ethanol (2 × 5 mL). The solution was concentrated, and the residue was washed several times with CH_2Cl_2 and THF. Finally, the product was precipitated out by dissolving it in MeOH and adding excess diethyl ether to furnish pure compound **46** (24 mg, 73%) as a white amorphous solid: mp 170−172 °C (dec); ^{1}H NMR (300 MHz, MeOH-d_4) δ 5.87 (s, 1 H), 5.46 (s, 1 H), 4.50−4.41 (m, 1 H), 3.96−3.92 (m, 1 H), 3.73−3.71 (m, 3 H), 3.64−3.61 (m, 2 H), 2.01 (s, 3 H); ^{13}C NMR (75 MHz, MeOH-d_4) δ 167.3, 160.8, 149.7, 144.2, 140.0, 119.8, 75.5, 73.2, 69.1, 68.6, 67.9, 65.7, 18.5; ESIMS m/z (rel. intensity) 368 (MNa[+], 100), 283 (13), 102 (27); negative ion ESIMS m/z (rel. intensity) 344 [M − H^{+}][−], 100], 325 (3), 210 (5); HRMS m/z calcd for $C_{13}H_{19}N_3O_8Na$ (MNa[+]) 368.1070, found 368.1073. Anal. Calcd for $C_{13}H_{19}N_3O_8$: C, 45.22; H, 5.55; N, 12.17. Found: C, 45.41; H, 5.27; N, 12.40.

N-(2,4-Dioxo-6-(((4S,4′R,5R)-2,2,2′,2′-tetramethyl-4,4′-bi-(1,3-dioxolan)-5-yl)methylthio)-1,2,3,4-tetrahydropyrimidin-5-yl)propionamide (48). Propionic acid (13 μL, 0.18 mmol), 1-ethyl-3-(3-dimethylaminopropyl) carbodiimide hydrochloride (23 mg, 0.12 mmol), and N-hydroxybenzotriazole monohydrate (16 mg, 0.12 mmol) were added to a solution of compound **47** (40 mg, 0.12 mmol) dissolved in pyridine (3.0 mL). The reaction mixture was stirred at rt for 12 h. The solvent was distilled off under reduced pressure, and the residue was dissolved in EtOAc (15 mL) and washed with water (2 × 15 mL). The organic layer was dried, and solvent was distilled off. The residue was purified by flash column chromatography with silica gel, eluting with 5% MeOH in ethyl acetate in hexane, to afford compound **48** (30 mg, 65%) as a colorless oil: ^{1}H NMR (300 MHz, MeOH-d_4) δ 4.45 (q, J = 6.1 Hz, 1 H), 4.20−4.07 (m, 3 H), 3.89 (dd, J = 4.7, 8.1 Hz, 1 H), 3.37−3.30 (m, 2 H), 2.38 (q, J = 7.6 Hz, 2 H), 1.46 (s, 3 H), 1.38 (s, 3 H), 1.35 (s, 3 H), 1.32 (s, 3 H), 1.19 (t, J = 7.6 Hz, 3 H); ^{13}C NMR (75 MHz, MeOH-d_4) δ 177.1, 162.5, 152.6, 152.0, 111.3, 110.8, 79.9, 79.1, 74.5, 68.8, 33.7, 29.8, 27.9, 27.1, 25.6, 25.4, 10.2; ESIMS m/z (rel. intensity) 468 (MK[+], 100), 452 (MNa[+], 29), 430 (MH[+], 5), 268 (13); negative ion ESIMS m/z (rel. intensity) 428 [(M − H^{+})[−], 100]; HRMS m/z calcd for $C_{18}H_{27}N_3O_7SNa$ (MNa[+]) 452.1467, found 452.1461. Anal. Calcd for $C_{18}H_{27}N_3O_7S$: C, 50.34; H, 6.34; N, 9.78; S, 7.47. Found: C, 50.46; H, 6.49; N, 9.81; S, 7.61.

N-(2,4-Dioxo-6-((2R,3R,4R)-2,3,4,5-tetrahydroxypentylthio)-1,2,3,4-tetrahydropyrimidin-5-yl)propionamide (49). HCl (1 N, 2 mL) was added to compound **48** (30 mg, 0.068 mmol) dissolved in MeOH (2 mL). The reaction mixture was stirred for 8 h at room temperature. The solution was concentrated, and the residue was washed several times with CH_2Cl_2 (3 × 10 mL) and THF (3 × 10 mL). Finally, compound **49** was precipitated out by dissolving it in MeOH and adding excess diethyl ether to furnish pure compound **49** (17 mg, 70%) as a white amorphous solid: mp 137−140 °C (dec); ^{1}H NMR (300 MHz, MeOH-d_4) δ 3.97−3.88 (m, 1 H), 3.78−3.72 (m, 3 H), 3.67−3.56 (m, 3 H), 2.35 (q, J = 7.5 Hz, 2 H), 1.19 (t, J = 7.5 Hz, 3 H); ^{13}C NMR (125 MHz, CDCl$_3$) δ 177.1, 169.5, 162.6, 158.2, 104.8, 73.3, 63.1, 33.3, 29.4, 9.2; ESIMS m/z (rel. intensity) 721 (2MNa[+], 94), 372 (MNa[+], 100), 350 (MH[+], 5); negative ion ESIMS m/z (rel. intensity) 348 [(M − H^{+})[−], 100]; HRMS m/z calcd for $C_{12}H_{19}N_3O_7SNa$ (MNa[+]) 372.0841, found 372.0843. Anal. Calcd for $C_{12}H_{19}N_3O_7S$: C, 41.25; H, 5.48; N, 12.03; S, 9.18. Found: C, 41.31; H, 5.48; N, 12.21; S, 9.31.

N-(2,4-Dioxo-6-(((4S,4′R,5R)-2,2,2′,2′-tetramethyl-4,4′-bi-(1,3-dioxolan)-5-yl)methylthio)-1,2,3,4-tetrahydropyrimidin-5-yl)methacrylamide (50). Methacrylic acid (13 μL, 0.15 mmol), 1-ethyl-3-(3-dimethylaminopropyl) carbodiimide hydrochloride (20 mg, 0.10 mmol), and N-hydroxybenzotriazole monohydrate (14 mg, 0.10 mmol) were added to a solution of compound **47** (35 mg, 0.10 mmol) dissolved in pyridine (3.0 mL). The reaction mixture was stirred at room temperature for 12 h. The solvent was distilled off under reduced pressure, and the residue was dissolved in EtOAc (15 mL) and washed with water (2 × 15 mL). The organic layer was dried, and solvent was distilled off. The residue was purified by flash column chromatography with silica gel, eluting with 5% MeOH in ethyl acetate in hexane, to afford compound **50** (28 mg, 68%) as a white amorphous solid: mp 95−98 °C; ^{1}H NMR (300 MHz, MeOH-d_4) δ 5.89 (s, 1 H), 5.52 (s, 1 H),

5.48 (s, 1 H), 4.45 (q, J = 6.1 Hz, 1 H), 4.18−4.07 (m, 3 H), 3.89 (dd, J = 4.7, 8.1 Hz, 1 H), 3.38−3.34 (m, 2 H), 2.15 (s, 3 H), 1.46 (s, 3 H), 1.37 (s, 3 H), 1.35 (s, 3 H), 1.32 (s, 3 H); ^{13}C NMR (75 MHz, MeOH-d_4) δ 170.9, 162.5, 153.1, 152.1, 140.8, 129.2, 121.9, 111.3, 110.8, 79.9, 79.0, 74.5, 68.8, 33.7, 27.9, 27.1, 25.6, 25.4, 18.8; ESIMS m/z (rel. intensity) 464 (MNa[+], 64), 442 (MH[+], 100), 166 (26); negative ion ESIMS m/z (rel. intensity) 440 [(M − H^{+})[−], 100]; HRMS m/z calcd for $C_{19}H_{28}N_3O_7S$ (MH[+]) 442.1648, found 442.1655. Anal. Calcd for $C_{19}H_{27}N_3O_7S$: C, 51.69; H, 6.16; N, 9.52; S, 7.26. Found: C, 51.92; H, 5.91; N, 9.60; S, 7.02.

N-(2,4-Dioxo-6-((2R,3R,4R)-2,3,4,5-tetrahydroxypentylthio)-1,2,3,4-tetrahydropyrimidin-5-yl)methacrylamide (51). HCl (1 N, 2 mL) was added to compound **50** (30 mg, 0.068 mmol) dissolved in MeOH (2 mL). The reaction mixture was stirred for 8 h at room temperature. The solution was concentrated, and the residue was washed several times with CH_2Cl_2 (3 × 10 mL) and THF (3 × 10 mL). Finally, compound **51** was precipitated out by dissolving in MeOH and adding excess diethyl ether to furnish pure compound **51** (19 mg, 78%) as a white amorphous solid: mp 140−143 °C (dec); ^{1}H NMR (300 MHz, MeOH-d_4) δ 5.88 (s, 1 H), 5.49 (s, 1 H), 3.99 (q, J = 6.1 Hz, 1 H), 3.78−368 (m, 2 H), 3.65−3.59 (m, 2 H), 3.30−3.27 (m, 2 H), 2.0 (s, 3 H); ^{13}C NMR (125 MHz, MeOH-d_4) δ 171.2, 163.8, 154.1, 141.0, 129.9, 121.7, 108.6, 74.7, 74.4, 74.0, 64.7, 35.9, 19.0; ESIMS m/z (rel. intensity) 745 (2MNa[+], 100), 384 (MNa[+], 48), 361 (MH[+], 14); negative ion ESIMS m/z (rel. intensity) 360 [(M − H^{+})[−], 100]; HRMS m/z calcd for $C_{13}H_{20}N_3O_7S$ (MH[+]) 361.1022, found 361.1025. Anal. Calcd for $C_{13}H_{19}N_3O_7S$: C, 43.21; H, 5.30; N, 11.63; S, 8.87. Found: C, 43.01; H, 5.44; N, 11.49; S, 9.03.

2,6-Dimethoxy-5-nitro-N-((2S,3S,4R)-2,3,4,5-tetrakis(tert-butyldimethylsilyloxy)-pentyl)pyrimidine-4-amine (53).[50] Compound **52** (5.2854 g, 15.8 mmol), tert-butyldimethylsilyl chloride (16.55 g, 109.8 mmol), and imidazole (7.49 g, 109.8 mmol) were dissolved in dry DMF (115 mL), and the mixture was stirred at room temperature for 2 days. DMF was then removed under reduced pressure, and the residue was stirred in ethyl acetate (90 mL) for 2 h. The precipitated salt was filtered, and the filtrate was concentrated to form a yellow oil, which was separated by silica gel flash column chromatography, eluting with hexane/EtOAc (95:5), to afford pure **53** (6.95 g, 57%) as a light yellow oil: ^{1}H NMR (300 MHz, CDCl$_3$) δ 9.00 (s, 1 H), 4.10−4.09 (m, 1 H), 4.06 (s, 3 H), 3.96 (s, 3 H), 3.93−3.88 (m, 2 H), 3.83−3.80 (dd, J = 2.57 Hz, J = 5.99 Hz, 1 H), 3.72−3.67 (dd, J = 5.16 Hz, J = 10.32 Hz, 1 H), 3.56−3.51 (m, 2 H), 0.87 (s, 9 H), 0.86 (s, 9 H), 0.85 (s, 9 H), 0.84 (s, 9 H), 0.11 (s, 3 H), 0.08 (s, 3 H), 0.06 (s, 6 H), 0.04 (s, 3 H), 0.03 (s, 6 H), −0.04 (s, 3 H); ESIMS (MH[+]) m/z 791. Anal. Calcd for $C_{35}H_{74}N_4O_8Si_4$: C, 53.12; H, 9.43; N, 7.08; Si, 14.20. Found: C, 52.89, H, 9.21; N, 7.34; Si, 13.93.

2,6-Dimethoxy-N⁴-((2S,3S,4R)-2,3,4,5-tetrakis(tert-butyldimethylsilyloxy)-pentyl)pyrimidine-4,5-diamine (54). Compound **53** (6.9 g, 8.73 mmol) was added to a methanol (175 mL) and water (10 mL) mixture. $Na_2S_2O_4$ (11.4 g, 65.4 mmol) was added to the reaction mixture. The mixture was heated at reflux and stirred for 6 h. The reaction mixture was then cooled to room temperature. The solution was filtered through Celite, and the filtrate was dried to afford a residue. The residue was separated by silica gel flash column chromatography with hexane/ethyl acetate 20:1 as the mobile phase to afford the product **54** as unstable yellow oil (6.24 g, 94%) that soon turned purple: ^{1}H NMR (300 MHz, CDCl$_3$) δ 4.03−3.98 (m, 1 H), 3.93−3.89 (m, 1 H), 3.90 (s, 3 H), 3.85 (s, 3 H), 3.84−3.80 (m, 1 H), 3.76−3.64 (m, 2 H), 3.57−3.45 (m, 2 H), 0.88−0.86 (m, 36 H), 0.10−0.00 (m, 24 H); ^{13}C NMR (75 MHz, CDCl$_3$) δ 161.2, 159.6, 159.1, 100.8, 75.0, 71.7, 64.7, 54.1, 53.6, 43.0, 31.6, 29.6, 26.1, 25.9, 25.3, 22.6, 18.4, 18.3, 18.2, 18.0, 14.1, −4.1, −4.3, −4.6, −4.7, −4.9, −5.3, −5.4; ESIMS (MH[+]) m/z 761. Anal. Calcd for $C_{35}H_{76}N_4O_6Si_4$: C, 55.21; H, 10.06; N, 7.36; Si, 14.76. Found: C, 55.58; H, 10.20; N, 7.14; Si, 14.40.

N-(2,4-Dimethoxy-6-((2S,3S,4R)-2,3,4,5-tetrakis(tert-butyldimethylsilyloxy)-pentylamino)pyrimidine-5-yl)methacrylamide (55). Compound **54** (3.28 g, 4.32 mmol) was mixed with THF (30 mL). Triethylamine (6.0 mL, 43.3 mmol) was added to the THF solution. The mixture was cooled to 0 °C, and methacryloyl chloride (678 mg, 6.48 mmol) was added dropwise. The reaction mixture was stirred at 0

°C for 0.5 h. The reaction mixture was warmed to room temperature and stirred for 20 min. The mixture was dried in vacuo to get a residue, and that was purified by silica gel flash column chromatography with hexane/ethyl acetate 20:1 as the mobile phase to afford the product **55** as a colorless oil (2.53 g, 71%): ^{1}H NMR (300 MHz, CDCl$_3$) δ 5.84 (s, 1 H), 5.58 (brs, 1 H), 5.45 (s, 1 H), 3.95 −3.91 (m, 2 H), 3.89 (s, 3 H), 3.88 (s, 3 H), 3.78−3.68 (m, 3 H), 3.57−3.51 (m, 1 H), 3.44−3.41 (m, 1 H), 2.06 (s, 3 H), 0.87−0.83 (m, 36 H), 0.08- −0.05 (m, 24 H); ^{13}C NMR (75 MHz, CDCl$_3$) δ 166.8, 164.3, 162.3, 139.4, 120.9, 94.5, 74.6, 71.6, 64.6, 54.4, 54.0, 43.3, 31.9, 31.6, 29.7, 26.1, 25.9, 22.6, 18.7, 18.4, 18.3, 18.2, 18.0, 14.1, −4.0, −4.3, −4.4, −4.6, −5.2, −5.3, −5.4; ESIMS (MH$^+$) m/z 829. Anal. Calcd for C$_{39}$H$_{80}$N$_4$O$_7$Si$_4$: C, 56.48; H, 9.72; N, 6.75; Si, 13.54. Found: C, 56.83; H, 9.40; N, 6.38; Si, 13.21.

N-[2,4-Dioxo-6-((2S,3S,4R)-2,3,4,5-tetrahydroxypentylamino]-1,2,3,4-tetrahydropyrimidin-5-yl)methacrylamide (56). Compound **55** (0.7 g, 0.85 mmol) was dissolved in a solution made from 48% HBr/H$_2$O (2:1, 30 mL) and MeOH (30 mL), and the mixture was stirred at 55−60 °C for 3 h. The solvent was removed in vacuo, the residue was dissolved in MeOH (10 mL), and ethyl ether (60 mL) was added. After 24 h in the refrigerator, the precipitate was filtered out as a light red solid, which was dissolved in water (60 mL), decolorized with active charcoal, and filtered. The solvent was removed from the filtrate, and the residue was purified by silica gel flash column chromatography (EtOAc/EtOH/H$_2$O/AcOH 67:23:9:1) twice and Sephadex LH 20 column twice with MeOH to remove silica gel and other inorganic impurities and provide the product **56** (100 mg, 34%) as a white semisolid powder: ^{1}H NMR (300 MHz, D$_2$O) δ 5.88 (s, 1 H), 5.55 (s, 1 H), 3.87−3.47 (m, 7 H), 1.95 (s, 3 H); ^{13}C NMR (125 MHz, D$_2$O) δ 172.4, 162.6, 153.6, 151.3, 138.1, 123.1, 86.3, 72.2, 72.1, 70.3, 62.3, 44.1, 17.7; ESIMS m/z (rel. intensity) 389 [(M2Na$^+$ − H$^+$)$^+$, 100], 367 (MNa$^+$, 76); HRMS calcd for C$_{13}$H$_{20}$N$_4$O$_7$Na (MNa$^+$) 367.1230, found 367.1226. Anal. Calcd for C$_{13}$H$_{20}$N$_4$O$_7$·1.5 H$_2$O·1 MeOH: C, 41.68; H, 6.75; N, 13.89. Found: C, 41.27; H, 6.35; N, 14.19.

N-(2,4-Bis(benzyloxy)-6-((2S,3S,4R)-2,3,4,5-tetrakis(*tert*-butyldimethylsilyloxy)pentylamino)pyrimidin-5-yl)-2-chloropropanamide (58). Compound **57** (210 mg, 0.23 mmol) was mixed with THF (5 mL). TEA (0.3 mL, 2.1 mmol) was added to the THF solution. The mixture was cooled to 0 °C, and 2-chloropropanoyl chloride (34 μL, 44 mg, 0.34 mmol) was added dropwise. The reaction mixture was stirred at 0 °C for 0.5 h. The mixture was dried in vacuo to yield a residue, and that was purified by silica gel flash column chromatography to provide the product **58** as a yellow oil (200 mg, 87%): ^{1}H NMR (300 MHz, CDCl$_3$) δ 7.48−7.26 (m, 10 H), 5.42−5.35 (m, 4 H), 4.08−3.65 (m, 7 H), 1.77−1.75 (d, J = 6.7 Hz, 3 H), 0.93−0.90 (m, 36 H), 0.15−0.01 (m, 24 H); ^{13}C NMR (75 MHz, CDCl$_3$) δ 168.9, 164.1, 162.1, 162.1, 160.3 160.2, 137.0, 136.5, 128.3, 128.2, 128.0, 127.8, 127.7, 127.6, 93.5, 93.4, 76.6, 74.5, 71.3, 68.8, 68.3, 64.5, 60.3, 55.7, 43.2, 26.0, 25.9, 22.7, 22.6, 18.4, 18.2, 18.1, 17.9, 14.1; ESIMS m/z (rel. intensity) 1005.32 [M(Cl^{37})H$^+$, 64.10], 1003.34 [M(Cl^{35})H$^+$, 100]; HRMS calcd for C$_{50}$H$_{88}$ClN$_4$O$_7$Si$_4$ (MH$^+$) 1003.5419, found 1003.5408. Anal. Calcd for C$_{50}$H$_{87}$ClN$_4$O$_7$Si$_4$: C, 59.81; H, 8.73; N, 5.58; Si, 11.19. Found: C, 60.03; H, 8.97; N, 5.61; Si, 11.25.

N-(2,4-Bis(benzyloxy)-6-((2S,3S,4R)-2,3,4,5-tetrahydroxypentylamino)pyrimidin-5-yl)-2-chloropropanamide (59). Compound **58** (144 mg, 0.14 mmol) was mixed with THF (7 mL). TBAF (1.0 M tetra-n-butylammonium fluoride in THF, 0.65 mmol, 0.65 mL) was added to the reaction mixture. The mixture was stirred at room temperature for 4 h and then dried in vacuo to afford a residue. The residue was purified by silica gel preparative TLC (solvent system: EtOAc/MeOH 20:1) to give a white solid **59** (65 mg, 83%): mp 132−134 °C; ^{1}H NMR (300 MHz, MeOH-d_4) δ 7.33−7.17 (m, 10 H), 5.24−5.21 (d, J = 8.2 Hz, 4 H), 4.53−4.46 (q, J = 6.8, 13.7 Hz, 1 H), 3.80−3.42 (m, 7 H), 1.55−1.53 (d, J = 6.9 Hz, 3 H); ^{13}C NMR (75 MHz, MeOH-d_4) δ 172.9, 166.3, 163.8, 163.0, 138.5, 138.3, 129.4, 129.4, 129.0, 128.95, 128.9, 128.6, 94.1, 74.4, 74.2, 72.8, 70.0, 69.3, 64.6, 55.2, 44.8, 22.2; ESIMS m/z (rel. intensity) 549 [M(Cl^{37})H$^+$, 34], 547 [M(Cl^{35})H$^+$, 100]; HRMS calcd for C$_{26}$H$_{32}$ClN$_4$O$_7$ (MH$^+$) 547.1960, found 547.1959. Anal. Calcd for C$_{26}$H$_{31}$ClN$_4$O$_7$: C, 57.09; H, 5.71; N, 10.24. Found: C, 56.85; H, 5.49; N, 10.45.

2-Chloro-N-(2,4-dioxo-6-((2S,3S,4R)-2,3,4,5-tetrahydroxypentylamino)-1,2,3,4-tetrahydropyrimidin-5-yl)propanamide (60). Lindlar catalyst (5 mg) was added to a solution of compound **59** (50 mg, 0.13 mmol) in anhydrous ethanol (4 mL). 1,4-Cyclohexadiene (0.1 mL, 1.3 mmol) was added, and argon was bubbled through the reaction mixture for 10 min. The mixture was stirred at room temperature for 12 h. The reaction mixture was filtered through Celite, which was then washed with ethanol (2 × 5 mL). The solution was concentrated, and the residue was washed several times with CH$_2$Cl$_2$ and THF. Finally, compound **60** was precipitated out by dissolving it in MeOH and adding excess diethyl ether to furnish pure compound **60** (18 mg, 66%) as a white amorphous solid: mp 208−211 °C (dec); ^{1}H NMR (300 MHz, MeOH-d_4) δ 4.51 (q, J = 7.0, 13.7 Hz, 1 H), 3.75−3.72 (m, 1 H), 3.67−3.61 (m, 2 H), 3.54−3.46 (m, 2 H), 3.23−3.19 (m, 2 H), 1.18 (t, J = 7.6 Hz, 3 H); ^{13}C NMR (125 MHz, MeOH-d_4) δ 172.1, 161.8, 153.2, 150.7, 86.2, 72.9, 72.2, 71.5, 63.0, 54.0, 44.6, 20.6; ESIMS m/z (rel. intensity) 369 [M(Cl^{37})H$^+$, 32], 366 [M(Cl^{35})H$^+$, 100]; HRMS m/z calcd for C$_{12}$H$_{20}$ClN$_4$O$_7$ (MH$^+$) 367.1021, found 367.1023.

N-(2,4-Bis(benzyloxy)-6-((2S,3S,4R)-2,3,4,5-tetrakis(*tert*-butyldimethylsilyloxy)pentylamino)pyrimidin-5-yl)-2-chloroacetamide (61). Compound **57** (0.7 g, 0.77 mmol) was mixed with THF (20 mL). TEA (1 mL, 6.9 mmol) was added to the THF solution. The mixture was cooled to 0 °C, and 2-chloroacetyl chloride (88 μL, 121 mg, 1.1 mmol) was added dropwise. The reaction mixture was stirred at 0 °C for 0.5 h. The mixture was dried in vacuo to afford a residue that was purified by silica gel flash chromatography to provide the product **61** as a yellow oil (0.7 g, 92%): ^{1}H NMR (300 MHz, CDCl$_3$) δ 7.57 (s, 1 H), 7.45−7.26 (m, 10 H), 5.44−5.33 (m, 4 H), 4.14 (s, 2 H), 3.99−3.47 (m, 7 H), 0.92−0.88 (m, 36 H), 0.14−0.00 (m, 24 H); ^{13}C NMR (75 MHz, CDCl$_3$) δ 165.0, 164.0, 162.2, 160.1, 137.0, 136.6, 128.4, 128.3, 128.1, 127.9, 127.8, 127.5, 93.2, 74.5, 71.4, 68.9, 68.2, 64.4, 43.1, 42.5, 26.1, 26.1, 25.9, 18.4, 18.3, 18.2, 18.0, −4.0, −4.4, −4.4, −4.6, −5.2, −5.3, −5.4; ESIMS m/z (rel. intensity) 991 [M(Cl^{37})H$^+$, 63], 989 [M(Cl^{35})H$^+$, 100]; HRMS m/z calcd for C$_{49}$H$_{86}$ClN$_4$O$_7$Si$_4$ (MH$^+$) 989.5262, found 989.5269. Anal. Calcd for C$_{49}$H$_{85}$ClN$_4$O$_7$Si$_4$: C, 59.45; H, 8.65; N, 5.66; Si, 11.35. Found: C, 59.69; H, 8.73; N, 5.47; Si, 11.07.

N-(2,4-Bis(benzyloxy)-6-((2S,3S,4R)-2,3,4,5-tetrahydroxypentylamino)pyrimidin-5-yl)-2-chloroacetamide (62). Compound **61** (40 mg, 0.04 mmol) was mixed with THF (2 mL). TBAF (1.0 M tetra-n-butylammonium fluoride in THF, 0.2 mmol, 0.2 mL) was added to the reaction mixture. The mixture was stirred at room temperature for 4 h and then dried in vacuo to produce a residue. The residue was purified by silica gel preparative TLC (solvent system: EtOAc/MeOH 20:1) to yield a white solid **62** (17 mg, 79%): mp 130−131 °C; ^{1}H NMR (300 MHz, MeOH-d_4) δ 7.29−7.15 (m, 10 H), 5.25 (d, J = 15.0 Hz, 2 H), 5.18 (d, J = 15.2 Hz, 2 H), 4.09 (s, 2 H), 3.77−3.67 (m, 1 H), 3.66−3.40 (m, 6 H); ^{13}C NMR (75 MHz, MeOH-d_4) δ 169.9, 166.3, 163.8, 163.1, 138.5, 138.4, 129.4, 129.0, 128.8, 128.5, 94.0, 74.4, 74.2, 72.9, 70.0, 69.2, 64.6, 44.8, 43.3; ESIMS m/z (rel. intensity) 535 [M(Cl^{37})H$^+$, 36], 533 [M(Cl^{35})H$^+$, 100]; HRMS m/z calcd for C$_{25}$H$_{30}$ClN$_4$O$_7$ (MH$^+$) 533.1798, found 533.1803. Anal. Calcd for C$_{25}$H$_{29}$ClN$_4$O$_7$: C, 56.34; H, 5.48; N, 10.51. Found: C, 56.41; H, 5.61; N, 10.79.

2-Chloro-N-(2,4-dioxo-6-((2S,3S,4R)-2,3,4,5-tetrahydroxypentylamino)-1,2,3,4-tetrahydropyrimidin-5-yl)acetamide (63). Compound **62** (40 mg, 0.08 mmol) was mixed with anhydrous ethanol (5 mL). 1,4-Cyclohexadiene (130 mg, 1.6 mmol) and Pearlman's catalyst (40 mg, 20% Pd(OH)$_2$ on carbon) were added to the reaction mixture. The mixture was stirred at room temperature under argon for 18 h and then filtered. The filtrate was then dried in vacuo to yield a residue. The residue was purified by prep TLC (solvent system: EtOAc/EtOH/H$_2$O 15:5:2) to provide a white solid **63** (17 mg, 64%): mp 173−174 °C; ^{1}H NMR (500 MHz, D$_2$O) δ 4.25 (s, 2 H), 3.85−3.81 (m, 1 H), 3.75−3.69 (m, 2 H), 3.65−3.44 (m, 4 H); ^{13}C NMR (125 MHz, D$_2$O) δ 171.3, 162.5, 155.8, 153.2, 85.8, 72.19, 72.1, 70.5, 62.3, 43.8, 42.2; ESIMS m/z (rel. intensity) 353 [(M(Cl^{37}) − H$^+$)$^-$, 24,], 351 [(M(Cl^{35}) − H$^+$)$^-$, 100,]; HRMS calcd for C$_{11}$H$_{16}$ClN$_4$O$_7$ (M − H$^+$)$^-$ 351.0708, found 351.0707. Anal. Calcd for C$_{11}$H$_{17}$ClN$_4$O$_7$: C, 37.46; H, 4.86; N, 15.88. Found: C, 37.35; H, 4.61; N, 16.04.

N-(2,4-Bis(benzyloxy)-6-((2S,3S,4R)-2,3,4,5-tetrakis(*tert*-bu-tyldimethylsilyloxy)-pentylamino)pyrimidin-5-yl)-3,3,3-tri-fluoropropanamide (64). Compound **57** (0.58 mg, 0.64 mmol) was mixed with THF (15 mL). TEA (0.9 mL, 6.9 mmol) was added to the THF solution. The mixture was cooled to 0 °C, and 3,3,3-trifluoropropanoyl chloride (65 μL, 0.64 mmol) was added dropwise. The reaction mixture was stirred at 0 °C for 0.5 h. The mixture was dried in vacuo to provide a residue that was purified by silica gel flash chromatography to yield the product **64** as a yellow oil (0.49 mg, 75%): ^{1}H NMR (300 MHz, DMSO-d_6) δ 7.45−7.29 (m, 10 H), 5.78 (s, 1 H), 5.44−5.28 (m, 4 H), 4.03−4.01 (m, 1 H), 3.87−3.89 (m, 1 H), 3.76−3.69 (m, 2 H), 3.58−3.50 (m, 3 H), 3.40−3.37 (m, 2 H), 0.90−0.83 (m, 36 H), 0.13−0.02 (m, 24 H); ^{13}C NMR (75 MHz, CDCl$_3$) δ 164.11, 162.1, 161.7, 160.2, 136.9, 136.3, 128.6, 128.4, 128.2, 128.0, 127.8, 127.7, 129.3−118.3 (q, *J* = 275.6 Hz), 93.4, 74.7, 71.2, 69.2, 68.9, 68.4, 64.5, 43.3, 42.2−41.1 (q, *J* = 29.3 Hz), 26.0, 25.8, 18.3, 18.2, 18.1, 17.9, −4.1, −4.3, −4.4, −4.5, −4.7, −4.7, −5.3, −5.4, −5.5; ^{19}F NMR (300 MHz, CDCl$_3$) δ 16.9 (t, *J* = 11.7 Hz, 3 F); HRMS calcd for C$_{50}$H$_{86}$F$_3$N$_4$O$_7$Si$_4$ (MH$^+$) 1023.5526, found 1023.5519. Anal. Calcd for C$_{50}$H$_{85}$F$_3$N$_4$O$_7$Si$_4$: C, 58.67; H, 8.37; N, 5.47; Si, 10.98. Found: C, 58.83; H, 8.08; N, 5.40; Si, 11.15.

N-(2,4-Bis(benzyloxy)-6-((2S,3S,4R)-2,3,4,5-tetrahydroxypentylamino)pyrimidin-5-yl)-3,3,3-trifluoropro-panamide (65). Compound **64** (131 mg, 0.13 mmol) was mixed with THF (6 mL). TBAF (1.0 M tetra-*n*-butylammonium fluoride in THF, 0.58 mmol, 0.58 mL) was added to the reaction mixture. The mixture was stirred at room temperature for 4 h and then dried in vacuo to afford a residue. The residue was purified by silica gel preparative TLC (solvent system: EtOAc/MeOH 20:1) to produce a white solid **65** (61 mg, 84%): mp 137−138 °C; ^{1}H NMR (300 MHz, MeOH-d_4) δ 7.32−7.17 (m, 10 H), 5.25−5.23 (m, 4 H), 3.88−3.86 (m, 1 H), 3.78- 3.53 (m, 6 H), 3.37−3.30 (m, 2 H); ^{13}C NMR (75 MHz, MeOH-d_4) δ 166.3, 166.2, 163.8, 163.0, 138.5, 138.3, 129.4, 129.4, 129.0, 128.8, 128.6, 131.3−120.3 (q, *J* = 274.4 Hz), 94.0, 74.4, 74.2, 72.9, 70.0, 69.3, 64.6, 54.7, 44.8, 41.7−40.6 (q, *J* = 29.4 Hz); ^{19}F NMR (300 MHz, CDCl$_3$) δ 11.3 (t, *J* = 11.5 Hz, 3 F); HRMS calcd for C$_{26}$H$_{29}$F$_3$N$_4$O$_7$Na (MNa$^+$) 589.1886, found 589.1889. Anal. Calcd for C$_{26}$H$_{29}$F$_3$N$_4$O$_7$: C, 55.12; H, 5.16; N, 9.89. Found: C, 54.93; H, 5.23; N, 10.07.

N-(2,4-Dioxo-6-((2S,3S,4R)-2,3,4,5-tetrahydroxypentylami-no)-1,2,3,4-tetrahydropyrimidin-5-yl)-3,3,3-trifluoropropana-mide (66). Compound **65** (30 mg, 0.05 mmol) was mixed with anhydrous ethanol (3 mL). 1,4-Cyclohexadiene (80 mg, 1.0 mmol) and Pearlman's catalyst (30 mg, 20% Pd(OH)$_2$ on carbon) were added to the reaction mixture. The mixture was stirred at room temperature under argon for 24 h and then filtered. The filtrate was then dried in vacuo to yield a residue. The residue was purified by prep TLC (solvent system: EtOAc/EtOH/H$_2$O 15:5:2) to afford a white solid **66** (15 mg, 72%): mp 189−190 °C; ^{1}H NMR (500 MHz, D$_2$O) δ 3.84−3.83 (m, 1 H), 3.77−3.69 (m, 2 H), 3.61−3.54 (m, 4 H) 3.50−3.42 (m, 2 H); ^{13}C NMR (125 MHz, D$_2$O) δ 167.9, 162.4, 154.9, 152.5, 123.9 (q, *J* = 274.1 Hz), 85.9, 72.1, 70.3, 62.3, 43.8, 39.6 (q, *J* = 29.1 Hz); ^{19}F NMR (300 MHz, DMSO-d_6) δ 12.10 (t, *J* = 11.7 Hz, 3 F); HRMS (ESI) Calcd for C$_{12}$H$_{16}$F$_3$N$_4$O$_7$ (M − H$^+$)$^-$ 385.0971, found 385.0976. Anal. Calcd for C$_{12}$H$_{17}$F$_3$N$_4$O$_7$: C, 37.31; H, 4.44; N, 14.50. Found: C, 37.33; H, 4.67; N, 14.39.

N-(2,4-Bis(benzyloxy)-6-[(2S, 3S, 4R)-2,3,4,5-tetrakis(*tert*-bu-tyldimethy-silanyloxy)pentylamino]-pyrimidin-5-yl)-2-oxopro-panamide (67). Triethylamine (0.3 mL) was added to a solution of compound **57** (180 mg, 0.2 mmol) in THF (5 mL). The solution was cooled to 0 °C, and 2-oxopropanoyl chloride (24 μL, 0.24 mmol) was added dropwise. The reaction mixture was stirred at 0 °C for 12 h. The solvent was distilled off under reduced pressure, and the residue was dissolved in dichloromethane (20 mL) and washed with water (2 × 15 mL). The organic layer was dried, and solvent was distilled off. The residue was column chromatographed with flash silica gel, eluting with 35% ethyl acetate in hexane, to afford compound **67** (135 mg, 70%) as yellowish oil: ^{1}H NMR (300 MHz, CDCl$_3$) δ 8.21 (brs, 1 H), 7.43−7.24 (m, 10 H), 5.75 (m, 1 H), 5.42−5.27 (m, 4 H), 4.0 (m, 2 H), 3.88 (m, 2 H), 3.79 (m, 1 H), 3.59 (m, 1 H), 3.41 (m, 1 H), 2.47 (s, 3 H), 0.94 − 0.86 (m, 36 H), 0.20 −0.05 (m, 24 H); ^{13}C NMR (75 MHz, CDCl$_3$) δ 196.0, 163.7, 162.0, 159.2, 158.1, 137.0, 136.5, 128.5, 128.3, 128.1, 128.0,

127.7, 93.4, 74.5, 71.4, 68.9, 68.3, 64.5, 43.4, 26.14, 26.08, 25.9, 24.3, 18.4, 18.3, 18.2, 18.0, −4.0, −4.4, −4.5; ESIMS *m/z* (rel. intensity) 983 (MH$^+$, 100), 965 (11), 719 (16); negative ion ESIMS *m/z* (rel. intensity) 981 [(M − H$^+$)$^-$, 100], 911 (65), 847 (35); HRMS *m/z* calcd for C$_{50}$H$_{86}$N$_4$O$_8$Si$_4$ (MH$^+$) 983.5601, found 983.5609.

2,4-Bis(benzyloxy)-7-hydroxy-7-methyl-8-[(2S,3S,4R)-2,3,4,5-tetrahydroxypentyl]-7,8-dihydropteridin-6(5H)-one (68). Compound **67** (60 mg, 0.06 mmol) was dissolved in THF (3 mL), and TBAF (0.07 mL, 0.36 mmol, 1 M solution in THF) was added. The reaction mixture was stirred at room temperature for 8 h. THF was removed under vacuum. The residue was extracted with ethyl acetate (3 × 10 mL), washed with water (2 × 10 mL), dried with anhydrous Na$_2$SO$_4$, and concentrated under reduced pressure. The residue was column chromatographed with flash silica gel, eluting with 5% MeOH in ethyl acetate, to afford compound **68** (22 mg, 69%) as an oil: ^{1}H NMR (300 MHz, MeOH-d_4) δ 8.21 (brs, 1 H), 7.43−7.28 (m, 10 H), 5.43 (ABq, *J* = 8.4, 15.6 Hz, 2 H), 5.36 (s, 2 H), 4.18−4.10 (m, 1 H), 3.92−3.80 (m, 2 H), 3.81−3.51 (m, 4 H), 1.39 (s, 3 H); ^{13}C NMR (75 MHz, MeOH-d_4) δ 164.8, 170.0, 157.5, 150.6, 138.4, 137.9, 129.50, 129.46, 129.2, 128.94, 128.88, 126.1, 99.4, 90.8, 79.0, 74.2, 71.5, 70.1, 69.6, 64.7, 45.9, 24.5; ESIMS *m/z* (rel. intensity) 509 (MH$^+$ − H$_2$O, 56), 202 (100); negative ion ESIMS *m/z* (rel. intensity) 525 [(M − H$^+$)$^-$, 71], 507 [(M − H$^+$ − H$_2$O)$^-$, 100]; HRMS *m/z* calcd for C$_{26}$H$_{30}$N$_4$O$_8$ (M − H$^+$)$^-$ 525.1985, found 525.1984.

7-Hydroxy-7-methyl-8-[(2S,3S,4R)-2,3,4,5-tetrahydroxypen-tyl]-7,8-dihydropteridin-2,4,6(1H,3H,5H)-trione (69). Lindlar catalyst (5 mg) was added to a solution of compound **68** (20 mg, 0.04 mmol) in MeOH/EtOAc (3 + 1 mL). A hydrogen balloon was attached, and the mixture was stirred at room temperature for 12 h. The reaction mixture was filtered through Celite, which was then washed with 50% aq MeOH (5 mL). The solution was concentrated, and the residue was washed several times with CH$_2$Cl$_2$ (3 × 10 mL) and THF (3 × 10 mL). Finally, compound **69** was precipitated out by dissolving in MeOH and adding excess diethyl ether to furnish pure compound **69** (10 mg, 77%) as a white amorphous solid: mp 180−183 °C (dec); ^{1}H NMR (300 MHz, MeOH-d_4) δ 4.20−4.17 (m, 1 H), 4.07−4.01 (m, 1 H), 3.87−3.84 (m, 1 H), 3.77−3.74 (m, 1 H), 3.66−3.54 (m, 3 H), 1.40 (s, 3 H); ^{13}C NMR (125 MHz, MeOH-d_4) δ 164.2, 159.0, 152.5, 141.1, 95.4, 91.9, 79.8, 74.3, 71.2, 64.8, 48.2, 23.8; negative ion ESIMS *m/z* (rel. intensity) 345 [(M − H$^+$)$^-$, 10], 327 [(M − H$^+$ − H$_2$O)$^-$, 100]; negative ion HRMS *m/z* calcd for C$_{12}$H$_{17}$N$_4$O$_8$ (M − H$^+$)$^-$ 345.1046, found 345.1051. Anal. Calcd for C$_{12}$H$_{18}$N$_4$O$_8$·1.75H$_2$O: C, 38.15; H, 5.74; N, 14.83. Found: C, 37.82; H, 5.79; N, 14.42.

N-(6-Chloro-2,4-dioxo-1,2,3,4-tetrahydropyrimidin-5-yl)-methacrylamide (78). Lindlar catalyst (5 mg) was added to a solution of compound **80** (40 mg, 0.097 mmol) in anhydrous ethanol (4 mL). 1,4-Cyclohexadiene (53 μL, 0.97 mmol) was added, and argon was bubbled through the reaction mixture for 10 min. The mixture was stirred at room temperature for 12 h. The reaction mixture was filtered through Celite, which was then washed with ethanol (2 × 5 mL). The solution was concentrated. The residue was washed several times with CH$_2$Cl$_2$ and THF. Finally, compound **78** was precipitated out by dissolving it in MeOH and adding excess diethyl ether to furnish pure compound **78** (14 mg, 63%) as a white amorphous solid: mp 234−236 °C; ^{1}H NMR (300 MHz, MeOH-d_4) δ 5.89 (s, 1 H), 5.53 (s, 1 H), 1.99 (s, 3 H); ^{13}C NMR (75 MHz, MeOH-d_4) δ 170.9, 162.8, 151.3, 146.0, 140.6, 122.2, 110.4, 18.7; ESIMS *m/z* (rel. intensity) 252 (MNa$^+$, 100), 230 (MH$^+$, 4); negative ion ESIMS *m/z* (rel. intensity) 228 [(M − H$^+$)$^-$, 100], 192 (32); HRMS *m/z* calcd for C$_8$H$_8$ClN$_3$O$_3$Na (MNa$^+$) 252.0152, found 252.0153. Anal. Calcd for C$_8$H$_8$ClN$_3$O$_3$·0.5 MeOH: C, 41.56; H, 4.10; N, 17.11. Found: C, 41.13; H, 4.01; N, 16.80.

N-[2,4-Bis(dibenzyloxy)-6-chloropyrimidin-5-yl]-methacrylamide (80). Triethylamine (0.3 mL, 2.2 mmol) was added to a solution of compound **79** (80 mg, 0.23 mmol) in THF (5 mL). The solution was cooled to 0 °C, and methacrolyl chloride (28 μL, 0.28 mmol) was added dropwise. The reaction mixture was stirred at 0 °C for 12 h. The solvent was distilled off under reduced pressure, and the residue was dissolved in dichloromethane (20 mL) and washed with water (2 × 15 mL). The organic layer was dried and solvent was distilled off. The residue was flash column chromatographed with silica gel,

eluting with 35% ethyl acetate in hexane, to afford compound **80** (70 mg, 73%) as white semisolid: ^{1}H NMR (300 MHz, CDCl$_3$) δ 7.27–7.15 (m, 10 H), 5.63 (s, 1 H), 5.24 (s, 1 H), 5.21 (m, 4 H), 1.81 (s, 1 H); ^{13}C NMR (75 MHz, CDCl$_3$) δ 167.0, 166.8, 161.2, 158.6, 139.3, 135.5, 135.3, 128.3, 128.1, 127.5, 120.8, 110.4, 69.9, 69.4, 18.5; ESIMS *m/z* (rel. intensity) 432 (MNa$^+$, 100), 410 (MNa$^+$, 34) 268 (13); HRMS *m/z* calcd for C$_{22}$H$_{21}$ClN$_3$O$_3$Na (MH$^+$) 432.1091, found 432.1090. Anal. Calcd for C$_{22}$H$_{20}$ClN$_3$O$_3$: C, 64.47; H, 4.92; N, 10.25. Found: C, 64.22; H, 5.03; N, 9.94.

Computational Detail. The crystal structure of *M. tuberculosis* lumazine synthase and ligand **70** complex was obtained from the Protein Data Bank (PDB code: 2VI5).[48] To minimize the size of our simulation system, only one catalysis unit of lumazine synthase was kept, including subunit A, subunit B, inorganic phosphate, ligand **70**, and all surrounding crystal water. The complex structure of *M. tuberculosis* lumazine synthase with other ligands (**36, 69, 73,** and **81**) was built using 2VI5 as the template, followed by an energy minimization to optimize their geometry.

MD Simulations. All simulations were performed using AMBER 9.0. MD simulations were carried out using the parm99 force field at 300 K. An explicit solvent model TIP3P water was used, and the complexes were solvated with a truncated octahedron periodic box, extended to 8 Å from the solute atoms. Sodium ions were added as counterions to neutralize the system. For each ligand, the force field parameters were taken from the general Amber force field (GAFF), whereas the atomic partial charges were derived by geometry optimization using Gaussian 03 package[58] at Hartree–Fock (HF)/6-31G* level and subsequent single-point calculation of the electrostatic potential, to which the charges were fitted using the RESP procedure.

Prior to MD simulations, two steps of minimization were carried out; in the first stage, both protein and ligand were kept fixed with a constraint of 500 kcal/mol, and the positions of the water molecules were minimized; then in the second stage, the entire system without any constraint was minimized. The two minimization stages consisted of 3000 steps in which the first 1000 were steepest descent (SD) and the last 2000 conjugate gradient (CG). Molecular dynamics trajectories were run using the minimized structure as a starting input. The time step of the simulations was 2.0 fs with a cutoff of 10 Å for the nonbonded interaction, and SHAKE was employed to keep all bonds involving hydrogen atoms rigid. Constant volume was carried out for 100 ps, during which the temperature was raised from 0 to 300 K (using the Langevin dynamics method); then 1000 ps of constant-pressure MD were carried out at 300 K. The final structure of the complexes was obtained as the average of the last 400 ps of MD minimized with the CG method until a convergence of 0.05 kcal/mol·Å.

Energy Evaluation. To calculate the binding free energy, we extracted 100 snapshots (at time intervals of 4 ps) for each species (complex, receptor, and ligand) from the last 400 ps of MD of the ligand–lumazine synthase complexes. The binding free energies were calculated using the MM-PBSA method.[57] The binding affinity for a protein/ligand complex corresponds to the free energy of association in solution as shown in

$$\Delta G_{\text{bind}} = G_{\text{complex}} - (G_{\text{unbound protein}} + G_{\text{free ligand}}) \tag{1}$$

In MM-PBSA, the binding affinity in eq 1 is typically calculated using

$$\Delta G_{\text{bind}} = \Delta E_{\text{MM}} - (\Delta G_{\text{solv}} + T\Delta S_{\text{solute}}) \tag{2}$$

where ΔE_{MM} represents the change in molecular mechanics potential energy upon formation of the complex, calculated using all bonded and nonbonded interactions. Solvation free energy, ΔG_{solv}, is composed of the electrostatic component (G_{PB}) and a nonpolar component (G_{np}):

$$\Delta G_{\text{solv}} = \Delta G_{\text{PB}} + \Delta G_{\text{np}} \tag{3}$$

G_{PB} was calculated using the DelPhi program with PARSE radii. The cubic lattice had a grid spacing of 0.5 Å. Dielectric constants of 1 and 80 were used for the interior and exterior, respectively, and 1000 linear iterations were performed. The hydrophobic contribution to the solvation free energy, G_{np}, was calculated using the solvent-accessible

surface area (SASA) from the MSMS program, where $\gamma = 0.00542$ kcal/(mol·Å^2) and $\beta = 0.92$ kcal/mol with a solvent probe radius of 1.4 Å:

$$\Delta G_{\text{np}} = \Delta\text{SASA} + \beta \tag{4}$$

$T\Delta S_{\text{solute}}$ represents the entropic contribution to binding affinity at temperature T. The five ligands used in our calculation are structurally very similar analogues. For a series of compounds with similar structures and binding modes, the entropy contribution can be omitted if one is only interested in relative binding affinities. Since this calculation converges slowly and can have large uncertainties, we omitted the entropic contribution in this study.

Kinetic Assay of Lumazine Synthase Inhibitors. Assay mixtures contained 100 mM Tris hydrochloride, pH 7.0, 100 mM NaCl, 2% (v/v) DMSO, 5 mM dithiothreitol, 100 μM **2**, 0.3–2.0 μM lumazine synthase, variable concentrations of **1** (3–100 μM), and inhibitor (0–200 μM) in a volume of 0.2 mL. Assay mixtures were prepared as follows. A solution (176 μL) containing 100 mM NaCl, 5.0 mM dithiothreitol, 112 μM **2**, 0.34–2.3 μM lumazine synthase in 100 mM Tris hydrochloride, pH 7.0, was added to 4 μL of inhibitor in 100% (v/v) DMSO in a well of a 96-well microtiter plate. The reaction was started by adding 20 μL of a solution containing 100 mM NaCl, 5.0 mM dithiothreitol, and substrate **1** (30–1000 μM) in 100 mM Tris hydrochloride, pH 7.0. The formation of 6,7-dimethyl-8-D-ribityllumazine (**3**) was measured online for a period of 30 min at 27 °C with a computer-controlled plate reader at 408 nm ($\varepsilon_{\text{Lumazine}} = 10\,200$ M^{-1} cm^{-1}).

Kinetic Assay of Riboflavin Synthase Inhibitors. Assay mixtures contained 100 mM Tris hydrochloride, pH 7.0, 100 mM NaCl, 2% (v/v) DMSO, 5 mM dithiothreitol, 0.2–1 μM riboflavin synthase, variable concentrations of **3** (3–60 μM), and inhibitor (0–200 μM) in a volume of 0.2 mL. Assay mixtures were prepared as follows. A solution (176 μL) containing 100 mM NaCl, 5.0 mM dithiothreitol, 0.23–1.13 μM riboflavin synthase in 100 mM Tris hydrochloride, pH 7.0, was added to 4 μL of inhibitor in 100% (v/v) DMSO in a well of a 96-well microtiter plate. The reaction was started by adding 20 μL of a solution containing 100 mM NaCl, 5.0 mM dithiothreitol, and substrate **3** (30–600 μM) in 100 mM Tris hydrochloride, pH 7.0. The formation of riboflavin (**4**) was measured online for a period of 30 min at 27 °C with a computer-controlled plate reader at 470 nm ($\varepsilon_{\text{Riboflavin}} = 9600$ M^{-1} cm^{-1}).

Evaluation of Kinetic Data. The velocity–substrate data were fitted for all inhibitor concentrations with a nonlinear regression method using the program DynaFit.[60] Different inhibition models were considered for the calculation. K_i and K_{is} values ± standard deviations were obtained from the fit under consideration of the most likely inhibition model.

■ ASSOCIATED CONTENT

ⓢ Supporting Information

All experimental procedures and data, ^{1}H NMR and ^{13}C NMR spectra, and computational methods. This material is available free of charge via the Internet at http://pubs.acs.org.

■ AUTHOR INFORMATION

Corresponding Author

*Tel: 765-494-1465. Fax: 765-494-6790. E-mail: cushman@purdue.edu.

Notes

The authors declare no competing financial interest.

■ ACKNOWLEDGMENTS

■ REFERENCES

(1) Wang, A. *I Chuan Hsueh Pao* **1992**, *19*, 362.

(2) Oltmanns, O.; Lingens, F. *Z. Naturforsch.* **1967**, *22b*, 751.

(3) Logvinenko, E. M.; Shavlovsky, G. M. *Mikrobiologiya* **1967**, *41*, 978.

(4) Neuberger, G.; Bacher, A. *Biochem. Biophys. Res. Commun.* **1985**, *127*, 175.

(5) Rollenhagen, C.; Bumann, D. *Infect. Immun.* **2006**, *74*, 1649.

(6) Becker, D.; Selbach, M.; Rollenhagen, C.; Ballmaier, M.; Meyer, T. F.; Mann, M.; Bumann, D. *Nature* **2006**, *440*, 303.

(7) Fischer, M.; Bacher, A. *Nat. Prod. Rep.* **2005**, *22*, 324.

(8) Fischer, M.; Bacher, A. *Physiol. Plant.* **2006**, *126*, 304.

(9) Foor, F.; Brown, G. M. *J. Biol. Chem.* **1975**, *250*, 3545.

(10) Foor, F.; Brown, G. M. *Methods Enzymol.* **1980**, *66*, 303.

(11) Burrows, R. B.; Brown, G. M. *J. Bacteriol.* **1978**, *136*, 657.

(12) Hollander, I.; Brown, G. M. *Biochem. Biophys. Res. Commun.* **1979**, *89*, 759.

(13) Nielsen, P.; Bacher, A. *Biochem. Biophys. Acta* **1981**, *662*, 312.

(14) Richter, G.; Krieger, C.; Volk, R.; Kis, K.; Ritz, H.; Gotze, E.; Bacher, A. *Methods Enzymol.* **1997**, *280*, 374.

(15) Fischer, M.; Romisch, W.; Saller, S.; Illarionov, B.; Richter, G.; Rohdich, F.; Eisenreich, W.; Bacher, A. *J. Biol. Chem.* **2004**, *279*, 36299.

(16) Fischer, M.; Romisch, W.; Schiffmann, S.; Kelly, M.; Oschkinat, H.; Steinbacher, S.; Huber, R.; Eisenreich, W.; Richter, G.; Bacher, A. *J. Biol. Chem.* **2002**, *277*, 41410.

(17) Volk, R.; Bacher, A. *J. Am. Chem. Soc.* **1988**, *110*, 3651.

(18) Volk, R.; Bacher, A. *J. Biol. Chem.* **1990**, *265*, 19479.

(19) Neuberger, G.; Bacher, A. *Biochem. Biophys. Res. Commun.* **1986**, *139*, 1111.

(20) Kis, K.; Volk, R.; Bacher, A. *Biochemistry* **1995**, *34*, 2883.

(21) Fischer, M.; Haase, I.; Feicht, R.; Schramek, N.; Kohler, P.; Schieberle, P.; Bacher, A. *Biol. Chem.* **2005**, *386*, 417.

(22) Gerhardt, S.; Schott, A.-K.; Kairies, N.; Cushman, M.; Illarionov, B.; Eisenreich, W.; Bacher, A.; Huber, R.; Steinbacher, S.; Fischer, M. *Structure* **2002**, *10*, 1371.

(23) Illarionov, B.; Eisenreich, W.; Bacher, A. *Proc. Natl. Acad. Sci. U.S.A.* **2001**, *98*, 7224.

(24) Illarionov, B.; Eisenreich, W.; Schramek, N.; Bacher, A.; Fischer, M. *J. Biol. Chem.* **2005**, *280*, 28541.

(25) Illarionov, B.; Kemter, K.; Eberhardt, S.; Richter, G.; Cushman, M.; Bacher, A. *J. Biol. Chem.* **2001**, *276*, 11524.

(26) Maley, G. F.; Plaut, G. W. E. *J. Biol. Chem.* **1959**, *234*, 641.

(27) Plaut, G. W. E. *J. Biol. Chem.* **1963**, *238*, 2225.

(28) Plaut, G. W. E.; Harvey, R. A. *Methods Enzymol.* **1971**, *18B*, 515.

(29) Wacker, H.; Harvey, R. A.; Winestock, C. H.; Plaut, G. W. E. *J. Biol. Chem.* **1964**, *239*, 3493.

(30) Kim, R.-R.; Illarionov, B.; Joshi, M.; Cushman, M.; Lee, C. Y.; Eisenreich, W.; Fischer, B.; Bacher, A. *J. Am. Chem. Soc.* **2010**, *132*, 2983.

(31) Meining, W.; Mörtl, S.; Fischer, M.; Cushman, M.; Bacher, A.; Ladenstein, R. *J. Mol. Biol.* **2000**, *299*, 181.

(32) Zhang, X.; Meining, W.; Cushman, M.; Haase, I.; Fischer, M.; Bacher, A.; Ladenstein, R. *J. Mol. Biol.* **2003**, *328*, 167.

(33) Zheng, Y. J.; Viitanen, P. V.; Jordan, D. B. *Bioorg. Chem.* **2000**, *28*, 89.

(34) Haase, I.; Fischer, M.; Bacher, A.; Schramek, N. *J. Biol. Chem.* **2003**, *278*, 37909.

(35) Schramek, N.; Haase, I.; Fischer, M.; Bacher, A. *J. Am. Chem. Soc.* **2003**, *125*, 4460.

(36) Ritsert, K.; Huber, R.; Turk, D.; Ladenstein, R.; Schmidt-Bäse, K.; Bacher, A. *J. Mol. Biol.* **1995**, *253*, 151.

(37) Cushman, M.; Jin, G.; Illarionov, B.; Fischer, M.; Ladenstein, R.; Bacher, A. *J. Org. Chem.* **2005**, *70*, 8162.

(38) Zhang, Y. L.; Jin, G. Y.; Illarionov, B.; Bacher, A.; Fischer, M.; Cushman, M. *J. Org. Chem.* **2007**, *72*, 7176.

(39) Cushman, M.; Mihalic, J. T.; Kis, K.; Bacher, A. *J. Org. Chem.* **1999**, *64*, 3838.

(40) Morgunova, K.; Meining, W.; Illarionov, B.; Haase, I.; Jin, G.; Bacher, A.; Cushman, M.; Fischer, M.; Ladenstein, R. *Biochemistry* **2005**, *44*, 2746.

(41) Morgunova, E.; Illarionov, B.; Sambaiah, T.; Haase, I.; Bacher, A.; Cushman, M.; Fischer, M.; Ladenstein, R. *FEBS J* **2006**, *273*, 4790.

(42) Morgunova, E.; Saller, S.; Haase, I.; Cushman, M.; Bacher, A.; Fischer, M.; Ladenstein, R. *J. Biol. Chem.* **2007**, *282*, 17231.

(43) Yu, T. Y.; O'Connor, R. D.; Sivertsen, A. C.; Chiauzzi, C.; Poliks, B.; Fischer, M.; Bacher, A.; Haase, I.; Cushman, M.; Schaefer, J. *Biochemistry* **2008**, *47*, 13942.

(44) Ramsperger, A.; Augustin, M.; Schott, A. K.; Gerhardt, S.; Krojer, T.; Eisenreich, W.; Illarionov, B.; Cushman, M.; Bacher, A.; Huber, R.; Fischer, M. *J. Biol. Chem.* **2006**, *281*, 1224.

(45) Amoo, V. E.; Debernardo, S.; Weigele, M. *Tetrahedron Lett.* **1988**, *29*, 2401.

(46) Nutiu, R.; Boulton, A. J. *J. Chem. Soc., Perkin Trans. 1* **1976**, 1327.

(47) Sakamoto, T.; Uchiyama, D.; Kondo, Y.; Yamanaka, H. *Chem. Pharm. Bull.* **1993**, *41*, 478.

(48) Zhang, Y. L.; Illarionov, B.; Morgunova, E.; Jin, G. Y.; Bacher, A.; Fischer, M.; Ladenstein, R.; Cushman, M. *J. Org. Chem.* **2008**, *73*, 2715.

(49) Talukdar, A.; Illarionov, B.; Bacher, A.; Fischer, M.; Cushman, M. *J. Org. Chem.* **2007**, *72*, 7167.

(50) Cushman, M.; Sambaiah, T.; Jin, G.; Illarionov, B.; Fischer, M.; Bacher, A. *J. Org. Chem.* **2004**, *69*, 601.

(51) Chen, J.; Sambaiah, T.; Illarionov, B.; Fischer, M.; Bacher, A.; Cushman, M. *J. Org. Chem.* **2004**, *69*, 6996.

(52) Talukdar, A.; Morgunova, E.; Duan, J. X.; Meining, W.; Foloppe, N.; Nilsson, L.; Bacher, A.; Illarionov, B.; Fischer, M.; Ladenstein, R.; Cushman, M. *Bioorg. Med. Chem.* **2010**, *18*, 3518.

(53) Al-Hassan, S. S.; Kulick, R. J.; Livingston, D. B.; Suckling, C. J.; Wood, H. C. S.; Wrigglesworth, R.; Ferone, R. *J. Chem. Soc., Perkin Trans. 1* **1980**, 2645.

(54) Winestock, C. H.; Aogaichi, T.; Plaut, G. W. E. *J. Biol. Chem.* **1963**, *238*, 2866.

(55) Cushman, M.; Yang, D.; Kis, K.; Bacher, A. *J. Org. Chem.* **2001**, *66*, 8320.

(56) Kim, R.-R.; Illarionov, B.; Joshi, M.; Cushman, M.; Lee, C. Y.; Eisenreich, W.; Fischer, M.; Bacher, A. *J. Am. Chem. Soc.* **2010**, *132*, 2983.

(57) Kollman, P. A.; Massova, I.; Reyes, C.; Kuhn, B.; Huo, S. H.; Chong, L.; Lee, M.; Lee, T.; Duan, Y.; Wang, W.; Donini, O.; Cieplak, P.; Srinivasan, J.; Case, D. A.; Cheatham, T. E. *Acc. Chem. Res.* **2000**, *33*, 889.

(58) Frisch, M. J.; Trucks, G. W.; Schlegel, H. B.; Scuseria, G. E.; Robb, M. A.; Cheeseman, J. R.; Montgomery, J. A., Jr.; Vreven, T.; Kudin, K. N.; Burant, J. C.; Millam, J. M.; Iyengar, S. S.; Tomasi, J.; Barone, V.; Mennucci, B.; Cossi, M.; Scalmani, G.; Rega, N.; Petersson, G. A.; Nakatsuji, H.; Hada, M.; Ehara, M.; Toyota, K.; Fukuda, R.; Hasegawa, J.; Ishida, M.; Nakajima, T.; Honda, Y.; Kitao, O.; Nakai, H.; Klene, M.; Li, X.; Knox, J. E.; Hratchian, H. P.; Cross, J. B.; Adamo, C.; Jaramillo, J.; Gomperts, R.; Stratmann, R. E.; Yazyev, O.; Austin, A. J.; Cammi, R.; Pomelli, C.; Ochterski, J. W.; Ayala, P. Y.; Morokuma, K.; Voth, G. A.; Salvador, P.; Dannenberg, J. J.; Zakrzewski, V. G.; Dapprich, S.; Daniels, A. D.; Strain, M. C.; Farkas, O.; Malick, D. K.; Rabuck, A. D.; Raghavachari, K.; Foresman, J. B.; Ortiz, J. V.; Cui, Q.; Baboul, A. G.; Clifford, S.; Cioslowski, J.; Stefanov, B. B.; Liu, G.; Liashenko, A.; Piskorz, P.; Komaromi, I.; Martin, R. L.; Fox, D. J.; Keith, T.; Al-Laham, M. A.; Peng, C. Y.; Nanayakkara, A.; Challacombe, M.; Gill, P. M. W.; Johnson, B.; Chen, W.; Wong, M. W.; Gonzalez, C.; Pople, J. A. *Gaussian 03*, revision C.02 ed.; Gaussian, Inc.: Wallingford, CT, 2004.

(59) Talukdar, A.; Breen, M.; Bacher, A.; Illarionov, B.; Fischer, M.; Georg, G.; Ye, Q.-Z.; Cushman, M. *J. Org. Chem.* **2009**, *74*, 5123.

(60) Kuzmic, P. *Anal. Biochem.* **1960**, *237*, 260.